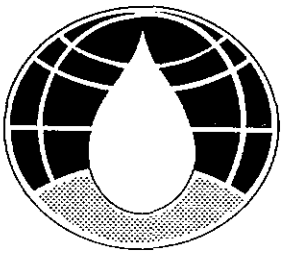

INTERNATIONAL
IRRIGATION
CENTER

OPTIMAL PERENNIAL GROUNDWATER YIELD PLANNING FOR THE EAST SHORE AREA, UTAH

by Shu Takahashi and
Richard C. Peralta

1992

Centro Internacional de Riegos Centro Internacional de Irrigação Centre International de l'Irrigation

Department of Agricultural and Irrigation Engineering
Utah State University, Logan, Utah 84322-4150, U.S.A., Telephone (801) 750-2800, Telex 3789426 UTAHSTATE U LOGN

OPTIMAL PERENNIAL GROUNDWATER YIELD PLANNING FOR THE EAST SHORE AREA, UTAH

by Shu Takahashi and Richard C. Peralta

Department of Biological and Irrigation Engineering

and

International Irrigation Center

Utah State University
Logan, UT 84322-4105
(801) 750-2785
FAX (801) 750-1248

REPORT IIC-92/3

Table of Contents

Abstract 2

Introduction 3

Relevant Research 5

The Study Area 9

Aquifer Simulation 12
Governing flow equation 12
USGS simulation model 13
Layered system 14
Model discretization 14
Boundary condition 15
Hydrogeological parameters 15

Embedding Simulation/Optimization (S/O) Model: a Modified Version of USUGWM 15
Model formulation 15
Objective function 16
Groundwater flow equation 16
Known constant recharge 17
Pumping and flowing wells 17
Pumping wells (gp) 18
Flowing wells (q^f) 18
Flow through general head boundary (q^g) 18
Evapotranspiration (q^e) 19
Drain discharge (q^d) 19
Vertical flow reduction (q^{rd}) 20
Bounds on variables 20
Difficulties in using the fully linearized formulas 20

Table of Contents (cont.)

Comparison of the original and modified USUGWMs 22
Linearized formula 22
Solution procedure 23
The original USUGWM 23
The modified USUGWM 24

Response Matrix Simulation/Optimization (S/O) Model 24
Generating influence coefficients 25
Model formulation 27

Preliminary Application Scenario to Response Matrix S/O Model 27
Bounds on variables 28
Bounds on pumping 28
Bounds on head in specific pumping cells 28
Bounds on head of the unconfined aquifer 28
Computation on head with Pre-ICG 29
Results from embedding and response matrix S/O models 29
Selection of S/O model for subsequent optimizations 30

Use of Embedding S/O Model for
Perennial-Yield Pumping Strategies 32
Bounds on pumping and head for management scenarios 33
Bounds on head 33
Bounds on pumping 33
Scenario 1: nonoptimal scenario 34
Scenario 2a: pumping from existing wells 34
Computated steady-state water budgets 34
Spatial distribution of pumping and flowing discharge 34
Scenario 2b: effects by changing
bounds on pumping and head 35
Upper bound on pumping 35
Lower bound on pumping 35
Maximum allowable drawdown 36
Scenario 2c: trade-off between pumping
and flowing discharge 36
Scenario 3a: pumping from proposed
wells along irrigation conveyance system 37
Computed steady-state water budgets 38
Spatial distribution of pumping and flowing discharge 38

Table of Contents (cont.)

Scenario 3b: assuring total discharge from wells 39
Scenario 4a: pumping from proposed
wells within water entities 40
Computed steady-state water budgets 40
Spatial distribution of pumping and flowing discharge 41
Scenario 4b: preventing salt water intrusion 41
Scenario 4c: egalitarian goal 42
Vertical water movement between layers 43
Declines of potentiometric heads in the lower layer 45
Validation of optimal solutions 45
Steady-state flow simulation 45
Evolution of head to the optimal steady-state 46
Global optimality 46

Summary and Conclusions 47

References 52

Authors History 55

List of Tables

Table 1. Number of finite-difference cells 56

Table 2. Comparison of model formulation: the embedding and response matrix approaches for preliminary problem 57

Table 3. Computational requirements of the embedding and response matrix models for preliminary problem 58

Table 4. Summary of model formulations for various scenarios 59

Table 5. Computed water budgets for Scenario 2b's 60

Table 6. Change in flow of flowing wells 61

Table 7. Spatial distribution of existing and additional pumping cells across the water entities 62

Table 8. Pumping and flowing well discharge for water entities for scenarios 3a and 3b 63

Table 9. Additional development of pumping under the egalitarian goal: scenario 4c 64

Table 10. Vertical water movements 65

List of Figures

Figure 1. Map of the East Shore Area, Utah 66

Figure 2. Generalized profile of the East Shore Area aquifer system 67

Figure 3. Change of potentiometric heads of layer 3 (lower layer) from 1955 to 1985 68

Figure 4. Discretization of layer 1 (upper layer) 69

Figure 5. Discretization of layer 2 (middle layer) 70

Figure 6. Discretization of layer 3 (lower layer) 71

Figure 7. Linear formulae for discharge from drains 72

Figure 8. Solving procedures for discharge from drains 73

Figure 9. Flow charts of solving procedures for the embedding and response matrix S/O models 74

Figure 10. Boundaries of water entities 75

Figure 11. Discharges for scenarios 1, 2a, 3a, 3b, 4a, and 4b 76

Figure 12. Tradeoff curve between pumping and flowing wells 77

Figure 13. Drawdown contours of scenario 1 78

Figure 14. Drawdown contours of scenario 2b (maximum allowable drawdown = 30 ft) 79

Figure 15. Drawdown contours of scenario 4b 80

Figure 16. Evolution of heads to the optimal steady-state 81

OPTIMAL PERENNIAL GROUNDWATER YIELD PLANNING FOR THE EAST SHORE AREA, UTAH

by Shu Takahashi[a] and Richard C. Peralta[b]

[a] Engineer, Nippon Koei Co. Ltd. and Graduate Student, Department of Biological and Irrigation Engineering, Utah State University, Logan, Utah 84322-4105.

[b] Professor, Department of Biological and Irrigation Engineering, Utah State University, Logan, Utah 84322-4105.

ABSTRACT

Computer models are developed for computing optimal perennial groundwater withdrawal strategies for the East Shore Area of Utah's Great Salt Lake. The underlying aquifer has three confined or unconfined layers. Both embedding and response matrix (RM) approaches are tested and compared. Historically, it has been difficult to incorporate simulation of an unconfined aquifer and many external flow equations described by nonsmooth functions within linear programming models. RM models normally assume system linearity. The presented RM model overcomes this difficulty using cycling and influence coefficients generated with a modified MODFLOW model. In this groundwater flow simulation model, the above nonlinear terms are treated linearly. The embedding model contains quasi-three-dimensional finite-difference forms of the groundwater flow equation as constraints. To achieve a stable optimal solution, the completely linearized formulation is cyclically optimized. The embedding model is preferred here because of its flexibility and ability to handle more linear and nonlinear hydrological variables for a specified amount of memory. Using the embedding model, optimal, spatially distributed, sustainable, annual groundwater pumping rates are computed for alternative future scenarios. Strategy results are then verified using external steady-state and transient simulation. This study demonstrates utility of the embedding approach for optimizing perennial-yield planning of large, complex aquifers.

INTRODUCTION

Long-term planning and management decisions can be facilitated by using combined simulation and optimization models which optimize steady (sustainable) groundwater extraction rates. Such regional groundwater planning models are constructed for the East Shore Area of Utah. There, the water demand for municipal and industrial use (M&I) is increasing due to urbanization. Increased groundwater extraction will decrease flow from flowing (artesian) wells.

This study started from applying a linear version of the USUGWM, developed by Gharbi et al.[11], to the East Shore Area aquifer system (three-layer, 4,880 cells). The USUGWM is the first embedding model to successfully optimize groundwater pumping for a large, complex, and nonlinear system. When the linear USUGWM is applied to a nonlinear system, heads known from the previous cycle are used to compute transmissivity and to select the linear segment of a nonsmooth function. The model is cyclically optimized until the values of variables do not change with the cycles. However, since the discretized system of this study area is extremely large and contains around 2,000 nonsmooth functions, the initial embedding model faced the following problems. The model contains about 40,000 nonzero elements and 12,000 single equations and variables. Using the previous version of MINOS on the VAX 6250, it took around 30 cycles and totaled around 12 hr CPU time to perform one optimization on the average. In cells containing nonsmooth functions, the bounds on head in the current cycle

are limited within those in the previous cycle. In this process, the solutions are sometimes declared to be infeasible during cycles even if the feasible solutions exist.

Because the embedding model always needs a specific amount of memory, the response matrix model can be an alternative. However, it is difficult to satisfy the system linearity while accurately representing the above nonlinear problems.

The objectives of this study are: (1) to improve the modelling approach originally presented in USUGWM to directly achieve an optimal solution without many cycles, (2) to develop the response matrix model to be suitable for nonlinear flow systems containing nonsmooth functions as well as transmissivity in an unconfined aquifer, and (3) to apply the appropriate model to develop perennial-yield pumping strategies for the study area.

Three management scenarios and their variations are implemented. After applying and comparing both the embedding and response matrix approaches for one scenario, the embedding approach was selected for one subsequent application. The major reason was its greater ability to handle numerous external flows as variables in the optimization scheme. Perennial-yield pumping strategies are computed for alternative future scenarios to demonstrate the flexible abilities of the embedding model. This model can help future water resource planning for the East Shore Area.

RELEVANT RESEARCH

A common management goal in arid and semi-arid regions is to fully utilize water resources to produce economic and social benefits. A groundwater management plan should satisfy specified objectives while considering the physical constraints of the aquifer system as well as legal and economic constraints. For the last two decades, groundwater development and conservation problems have been increasingly addressed using combined simulation and optimization (S/O) models. These combined models predict the behavior of a given aquifer and determine the best management strategy for the specified objectives and constraints.

Previous researchers have tackled a variety of groundwater management problems using several techniques. In general, most flow management models assumed system linearity. However, most real aquifer systems are complex and have nonlinear flow processes. Thus, there exists a need for an approach which can conveniently and accurately handle the common, nonlinear flows. Published research most relevant for this effort is cited below.

S/O models are frequently classified as using either the embedding approach or the response matrix approach, based on how groundwater head response to hydraulic stress is simulated in the model (see Ref. 13). The embedding approach incorporates finite-difference or finite-element approximations of the groundwater flow equation directly within the model as constraints. This approach provides

considerable information, such as optimal potentiometric head and pumping rate in each cell simultaneously for the whole area and for all time steps.

The embdding approach was first tested for groundwater managemet by Aguado and Remson[1]. Because of numerical difficulties with optimization algorithms resulting from the large dimensionality[13,32,33], the embedding approach was generally used for small scale, steady-state models. However, it has been more recently applied to larger scale problems. Cantiller et al.[6] used the embedding approach to develop a strategy for the conjunctive use of surface and groundwater for 13,000 square miles of the Mississippi alluvial, one-layer, large-scale aquifer system with 1,595 cells.

Gharbi et al.[11] used the embedding approach in the USU Groundwater Management Model (USUGWM) dealing with the 1,086 cell, two-layer (unconfined/confined), large-scale aquifer system underlying the Salt Lake Valley of Utah. In order to solve nonlinearities of unconfined flow, evapotranspiration, and aquifer-stream interflow, a cycling procedure was used. Before cycling begins, nonlinear formulas are linearized or quasi-linearized. Then optimization is performed. Because the optimization model uses a linear surrogate to a nonlinear formula, the model needs to be solved repeatedly until the values of variables updated in each repetition converge. This procedure has been used for several groundwater management models (e.g., Danskin and Gorelick[8], Peralta and Killian[25], Tung[31], and Willis and Yeh[35]). In general, the steady-state

embedding approach has been most useful for long-term perennial groundwater yield planning in an area where most cells contain pumping and many heads must be constrained.

Recently, a differential dynamic programming (DDP) algorithm has been used for groundwater management. Jones et al.[18] first applied this method to an unconfined aquifer system under transient conditions. Due to the use of decomposition, DDP can reduce the dimensionality problems associated with the embedding approach.

An alternative to the embedding approach is the response matrix approach, which is most commonly used for transient operational models. The response matrix approach uses superposition to compute heads and is appropriate for linear systems. Many researchers have used the response matrix approach for large-scale transient models. It does not require equations for all cells and time steps. It can calculate aquifer response at specified locations only. This reduces the need for computer memory. However, a preliminary simulation to generate influence coefficients using an external simulation model is necessary. Thus, any change in an aquifer parameter can require regenerating influence coefficients (see Refs. 13 and 26 for details). Influence coefficients are also termed discrete kernels[24,16], technological functions[3], algebraic technological functions[20], and response functions[34,31].

The Boussinesq equation for saturated groundwater flow is linear for a confined aquifer but is nonlinear for an

unconfined aquifer in which a saturated thickness varies significantly with head. The principle of superposition through influence coefficients cannot be applied to such a nonlinear system without adaptive measures or assumptions. Several researchers (e.g., Maddock[21], Heidari[15], Illangasekare and Morel-Seytoux[17], Danskin and Gorelick[8], Willis and Yeh[35], and Elwell and Lall[10]) have addressed this problem while using the response matrix approach. In this study, a different approach using cycling is demonstrated for perennial-yield planning in the East Shore Area aquifer system. This approach addresses the nonlinearity of flows described by nonsmooth functions as well as that of unconfined flow.

"Perennial yield" is defined as the maximum quantity of water that can be continuously withdrawn from a groundwater basin without adverse effect[2]. A "perennial-yield pumping strategy" is a specific pattern of spatially distributed pumping that causes the evolution and maintenance of an appropriate potentiometric surface. Thus a perennial-yield pumping strategy assures a certain amount of water to the user over a long time period. Such a perennial-yield pumping strategy can be computed using a steady-state S/O model. Knapp and Feinerman[19] endorsed the usefulness of computing optimal steady-state solutions.

If steady pumping is implemented and maintained, the potentiometric head of the aquifer will reach a certain level and, once achieved, will be maintained forever (discounting seasonal and daily changes, and assuming other recharge and

boundary conditions remain constant).

Based on the above review, none of the response matrix models explicitly address external flows described by nonsmooth functions such as evapotranspiration. Such flows are commonly assumed to be known (fixed) or their nonsmooth nature is ignored.

The discretized aquifer system of this study contains more cells than others reported in the literature. In this study, both embedding and response matrix approaches are improved in their ability to address external flows described by nonsmooth functions.

THE STUDY AREA

The East Shore Area, located north of Salt Lake City, is bounded by the Wasatch Front to the East and the Great Salt Lake to the West (Fig. 1). It is about 40 miles long and 3 to 20 miles wide, covering about 450 square miles. The population of the East Shore Area has tripled with the growth of agriculture, industry, and business during the last 40 years[27]. That portion of the study area from Willard to Farmington is the northern part of the most densely populated area in Utah.

To meet the increasing water demand in the area, the Weber Basin Project was implemented in 1952. This project utilizes the streamflow of the Weber River and the Ogden River with six dams and reservoirs and about 67 miles of conveyance systems. The project was designed to supply a total of

212,800 acre-ft per year, 162,800 acre-ft for irrigation and 50,000 acre-ft for municipal and industrial (M&I) use. The Weber Basin Conservancy District (Weber Basin W.C.D.) has since supplied water to this area. Recently, the United States Bureau of Reclamation (USBR) and the Weber Basin W.C.D.[30] proposed that the 33,000 acre-ft per year of water stored in Willard Reservoir should be converted from irrigation to M&I use.

Groundwater has been utilized for M&I use, irrigation, stock, watering, and domestic purposes in the area. Irrigated agriculture is the main user of the water and is mainly supplied from the Weber River. About 70% of the M&I use of water is supplied by groundwater[28,29]. Due to the rapid urbanization in the area for the last 20 years, the demand for M&I water has increased markedly, but the demand for irrigation water has been relatively constant. This trend is expected to continue.

The groundwater reservoir is a three-layer aquifer system. The upper layer is shallow and unconfined, the middle layer is partially unconfined, and the lower layer is deeply unconfined in the mountain side and confined near the Great Salt Lake. The generalized profile of the aquifer system in the East Shore Area is shown in Fig. 2. Along the mountain side, large pumping wells are utilized for municipal and industrial use[5]. Near the shore, the potentiometric heads of the middle and lower aquifers are above the ground surface. In addition, many flowing wells provide water for agriculture,

wetlands, and biota.

Groundwater levels in the East Shore Area have declined for more than 40 years. The decline exceeds 50 ft in the vicinity of Hill Air Force Base due to the increasing withdrawal of groundwater (Fig. 3). There was no significant decline of water quality of the aquifer between prior to 1970 and after 1980. Groundwater in most of the area is suitable for any use. However, groundwater in some areas, where chloride concentration exceeds 250 mg/l, is not recommended for public supply use and cannot be extensively developed[7]. Another concern about potential groundwater quality deterioration by agricultural pesticide use in the area has been recently reported[9]. The contamination hazard results because of the proximity of the water table to the ground surface, soil permeability and composition, and utilized chemicals.

Although a large amount of groundwater has been pumped near the mountains, water still moves upward through leakage from the underlying layers to the shallow and unconfined aquifer on the agricultural lands near the lake shore. Outflow from the aquifer into the Great Salt Lake still occurs[7].

The groundwater reservoir is expected to be able to contribute to the increasing demand for water in the East Shore Area. However, the following problems may result from improper groundwater management:

1. Pumping cost might increase or wells might become inoperable due to declining water levels.
2. Some flowing wells might not produce the flow needed for agriculture, wetlands, and wildlife.
3. Conflict among water users might cause societal problems.
4. Salt or brackish water might intrude from the Great Salt Lake.
5. Pesticides and insecticides on agricultural lands might degrade groundwater quality.

To address the above concerns, a combined model will be used to develop groundwater strategies for the study area. In that process, several innovations will be presented.

AQUIFER SIMULATION

Governing flow equation

A quasi-three-dimensional groundwater flow equation[22,12] for the multilayer system can be written as

$$\frac{\partial}{\partial x}\left(T_{xx}\frac{\partial h}{\partial x}\right) + \frac{\partial}{\partial y}\left(T_{yy}\frac{\partial h}{\partial y}\right) + VC_{l+1}\,(h_{l+1} - h_l) + VC_l\,(h_{l-1} - h_l) = W \qquad (1)$$

where

T_{xx} transmissivity along x coordinate axis (L^2/T);

T_{yy} transmissivitiy along y coordinate axis (L^2/T);

h potentiometric head or water table (L);

W volumetric flux per unit area and represents external flow (L/T);

VC_{l+1} hydraulic conductance between the upper layer l+1 and the layer l (L^2/T);

VC_l hydraulic conductance between the layer l and the lower layer l-1 (L^2/T);

USGS simulation model

Clark et al.[7] applied the McDonald and Harbaugh (MODFLOW) model to that part of the East Shore Area aquifer system from one mile north of Centerville to one mile north of Willard. Using geohydrological data and historical water-level and pumping records, they performed a steady-state calibration for 1955 conditions. Then they performed a transient calibration from 1955 to 1985. Results include the spatial distribution of transmissivities, storage coefficients, and several kinds of hydraulic conductances. After verification of the simulation model, the predictive simulations were performed for 1985 to 2005. Assumed are the normal recharge condition of 107,000 acre-ft or less-than-normal climatical condition of 100,000 acre-ft. By the year 2005, groundwater withdrawal rates are assumed to be twice the average of the 1980-1984 annual pumping from M&I wells of 23,400 acre-ft (a 25% increases each 5 years). Predicted are groundwater level declines of 35 ft and 50 ft in the pumping center near the Hill Air Force Base (Hill A.F.B.), assuming normal recharge conditions and less-than-normal recharge conditions, respectively. Also predicted was a decrease or a cessation of discharge from flowing wells.

General description of the USGS model is summarized as follows:

Layered system. Consistent with the generalized profile of the aquifer (Fig. 2), the USGS model consists of three layers. Layer 1 represents the upper, shallow, unconfined aquifer. This layer involves quasi-3d saturated flow under water table conditions, discharge from drains and flowing wells, evapotranspiration, and upward inflow from the underlying aquifer to the Great Salt Lake. Transmissivity of Layer 1 is treated as a function of head.

Layer 2, the middle layer, is partially unconfined and includes the "Sunset aquifer". Layer 3 represents the lowest aquifer which is deeply unconfined near the mountain side and confined under the rest of the entire area. Most of the large pumping wells for M&I use penetrate the "Delta aquifer" which is a principle part of the lower layer. In Layers 2 and 3, these transmissivities are assumed to be constant, even in the unconfined zone (no data for the case of the aquifer is available). Simulated are quasi-3d saturated flow under pressure, constant recharge, and discharge from flowing and pumping wells. Flow within aquitards between the aquifers is not simulated, but vertical flow through the aquitards is simulated.

Model discretization. The discretizations and cell types for Layers 1, 2, and 3 are shown in Figures 4, 5, and 6, respectively. A block-centered, finite-difference cell with a size length varying from 0.5 mile to 1.0 mile is used. The grid consists of 36 columns and 67 rows. The smallest active cells, representing 0.25 square mile, are used in the pumping

center near the Hill A.F.B. The largest active cells, containing 0.5 square mile, are primarily used in the Great Salt Lake. The number of each different type of cell is summarized in Table 1.

Boundary condition. The area is assumed to be surrounded by no-flow boundaries in every direction. On the west side, a general-head boundary is used to permit upward inflow from the underlying layers into the Great Salt Lake. It is assumed that this boundary condition will not change in the future.

Hydrogeological parameters. The distribution of hydrological parameters are determined based on the aquifer-test data. For example, transmissivity of Layer 3 ranges from less than 2,500 ft^2/day in the western part to 100,000 ft^2/day in the pumping center near Hill A.F.B.

EMBEDDING SIMULATION/OPTIMIZATION (S/O) MODEL :a MODIFIED VERSION of USUGWM

Model formulation

Most simply, the S/O model is formulated to maximize the perennial-yield groundwater pumping rate subject to the physical aquifer system. However, alternative management goals, involving political equity, tradeoffs between types of water users, and environmental protection are also considered. Thus, one additional objective function and several constraints are used. The model is written in the General Algebraic Modeling System GAMS language[4]. Optimization is performed with the MINOS[23] LP solver using an advanced simplex method.

Objective function. The objective function of the model is to maximize total groundwater extraction.

$$maximize \quad z = \sum_{o=1}^{N} gp_o \tag{2}$$

where

gp_o groundwater pumping in a cell o, (L^3/T);

N total number of cells with pumped wells.

Groundwater flow equation. The steady-state, finite-difference form of the quasi-three-dimensional groundwater flow equation (Eq. 1)[22] is contained directly as a constraint for every cell. Using the same form of equation permits validating the simulation abilities of the S/O model by using MODFLOW.

$$\begin{aligned} &CR_{l,i,j+1/2}(h_{l,i,j+1}-h_{l,i,j})+CR_{l,i,j-1/2}(h_{l.i,j-1}-h_{l.i,j}) \\ &+CC_{l,i+1/2,j}(h_{l,i+1,j}-h_{l,i,j})+CC_{l,i-1/2,j}(h_{l,i-1,j}-h_{l,i,j}) \\ &+CV_{l+1/2,i,j}(h_{l+1,i,j}-h_{l,i,j})+CV_{l-1/2,i,j}(h_{l-1,i,j}-h_{l,i,j}) \\ &= \Sigma^{N}_{n=1}\ q^{*}_{i,j,k,n} \end{aligned} \tag{3}$$

where

$$CR_{l,i,j+1/2}=2dx_j(T^j_{l,i,j}T^j_{l,i,j+1})/(T^j_{l,i,j}dy_{i+1}+T^j_{l,i,j+1}dy_i)$$

$$CC_{l,i+1/2,j}=2dy_i(T^i_{l,i,j}T^i_{l,i+1,j})/(T^i_{l,i,j}dx_{j+1}+T^i_{l,i+1,j}dx_j)$$

$$CV_{l+1/2,i,j}=dx_jdy_i/\{(dz_1/2Kz_{l,i,j})+(dz_{l+1}/2Kz_{l+1,i,j})\}$$

$h_{l,i,j}$ potentiometric head, (L);

l,i,j layer, row, column indices of a finite different cell;

CR,CC hydraulic conductance (harmonic averages of transmissivities) along x,y axes, (L^2/T);

CV vertical conductance between the nodes, (L^2/T);

$T_{l,i,j}$ transmissivity of a cell, (L^2/T); Transmissivity of unconfined layer is a function of head (T=kh). Transmissivity of confined layers is constant.

d_x, d_y, d_z cell sizes in layer l, row i, and column j, (L);

$Kz_{l,i,j}$ vertical hydraulic conductivity, (L^2/T);

$q^*_{l,i,j,n}$ (n th) external flow term in a cell, (L^3/T).

As in MODFLOW, several external flows are involved in the model as constraints.

Known constant recharge (q^r). The 1970-1984 average annual recharge rate of 10,700 acre-ft (normal climatic condition) is applied in the recharge area along the Wasatch Front (Figures 5 and 6). This includes bedrock recharge, unsaturated seepage from the Weber and Ogden Rivers, main canal seepage, precipitation, and irrigation seepage.

Pumping and flowing wells. Based on USGS work[7], about 5,900 wells have been constructed in the East Shore Area, including those in the city of Bountiful. There are 200 large diameter pumping wells for industrial and municipal use, 1,200 small diameter pumping wells for domestic, stock, and irrigation use, and 4,500 flowing wells for mainly irrigation use. Of the 4,500 flowing wells, 1,200 flow continuously and 1,800 are controlled by a pump or a valve. In addition, about

800 wells have been plugged or unused until 1985. There are also 700 wells which have ceased to flow because of a decrease in artesian pressure. Total annual discharge from wells in the area averaged about 54,000 acre-feet for 1969-1984. Of the total discharge 52% was extracted by large pumping wells, 41% was from continuous flowing wells, 3-6% from controlled flowing wells, and 2-4% from small diameter pumping wells.

Pumping wells (gp): The 1970-1984 average annual pumping rate of 23,400 acre-ft is considered via bounds in the S/O model. The existing pumping wells for M&I use are located at 61 cells in the middle and lower layers (Figures 5 and 6).

Flowing wells (q^f): To properly estimate the change in discharge from flowing wells on agricultural lands (Figures 5 and 6) and link it to the steady-state simulation and LP technique, discharge from the flowing wells is newly formulated as

$$q^f_{l,i,j} = \Gamma^f_{l,i,j} \, (h_{l,i,j} - h^{gs}_{l,i,j}) \quad \text{for } h_{l,i,j} \geq h^{gs}_{l,i,j}$$
$$= 0 \quad \text{for } h_{l,i,j} < h^{gs}_{l,i,j} \qquad (4)$$

where

Γ^f coefficient describing reduction in discharge rate of the flowing wells per 1 foot head decline, (L^2/T);

h^{gs} ground surface, (L).

Flow through general head boundary (q^g). Flow between the underlying aquifer and the Great Salt Lake is represented using a general-head boundary (Fig. 4).

$$q^g_{l,i,j} = \Gamma^g_{l,i,j} \, (h_{l,i,j} - h^{ls}_{l,i,j}) \qquad (5)$$

where

Γ^g hydraulic conductance between the aquifer and the general boundary head cell, (L^2/T);

h^{ls} water level of the Great Salt Lake, (L).

Evapotranspiration (q^e). Evapotranspiration on the agricultural or undeveloped lands of the upper layer (Fig. 4) is formulated as a function of water table elevation.

$$
\begin{aligned}
q^e_{l,i,j} &= E_o\, dx_j dy_i && \text{for } h_{l,i,j} \geq h^s_{l,i,j} \\
&= E_o\, dx_j dy_i \{h_{l,i,j} - (h^s_{l,i,j} - d_{l,i,j})\}/d_{l,i,j} \\
&\qquad \text{for } h^s_{l,i,j} - d_{l,i,j} \leq h_{l,i,j} < h^s_{l,i,j} \\
&= 0 && \text{for } h_{l,i,j} < h_{sl,i,j} - d_{l,i,j} \qquad (6)
\end{aligned}
$$

where

E^o potential evapotranspiration, (L/T);

h^s potentiometric surface elevation below which evapotranspiration decreases, (L);

d extinction depth, (L).

Drain discharge (q^d). There is considerable discharge from artificial and natural drains on the agricultural and undeveloped lands along the shore side (Fig. 4). This discharge is simulated as saturated flow using a function of water table elevation.

$$
\begin{aligned}
q^d_{l,i,j} &= \Gamma^d_{l,i,j}(h_{l,i,j} - B^d_{l,i,j}) && \text{for } h_{l,i,j} \geq B^d_{l,i,j} \\
&= 0 && \text{for } h_{l,i,j} < B^d_{l,i,j} \qquad (7)
\end{aligned}
$$

where

Γ^d hydraulic conductance between the aquifer and drains, (L^2/T);

B^d bottom elevation of the drains, (L).

Vertical flow reduction (q^{rd}). Eq. 3 overestimates the amount of vertical flow between layers when the lower layer becomes unconfined. In such cases, vertical flow must be reduced using Eq. 8. In this area, this correction (reduction) in flow only involves flow between the middle and lowest layers.

$$q^{rd}_{l,i,j} = -CV_{l,i,j}(E^{top}_{l+1,i,j}-h_{l,i,j}) \quad \text{for } h_{l+1,i,j}<E^{top}_{l+1,i,j}$$
$$= 0 \quad \text{for } h_{l+1,i,j} \geq E^{top}_{l+1,i,j} \quad (8)$$
$$(q^{rd}_{l,i,j}=-q^{rd}_{l+1,i,j})$$

where

E^{top}_{l+1} elevation of the top of layer l+1, (L).

Bounds on variables. Bounds on pumping and head are described as

$$gp^{L}_{l,i,j} \leq gp_{l,i,j} \leq gp^{U}_{l,i,j} \quad (9)$$

$$h^{L}_{l,i,j} \leq h_{l,i,j} \leq h^{U}_{l,i,j} \quad (10)$$

where

L and U notation of upper and lower bounds.

Difficulties in using the fully linearized formulas

The steady-state finite-difference form of the quasi-three-dimensional groundwater flow equation (Eq. 3) for the East Shore area contains (1) nonlinearity in an unconfined aquifer, where transmissivity is not constant but is a function of head and (2) nonsmooth functions of head consisting of two or three linear segments--evapotranspiration (q^e), discharge from flowing wells (q^f), drain discharge (q^d),

and vertical flow reduction due to desaturation (q^{rd}).

These terms cannot be solved with the LP technique directly. Following the procedure of USUGWM[11], the above terms are linearized first using known heads from the former cycle. Then, to reach the solution of the nonlinear system, the linearized model is rerun (cycled) until variable values do not change with the cycles.

A model for the East Shore Area can be formulated without making major changes to the USUGWM originally applied to the Salt Lake Valley[12]. Necessary changes include adding the expressing for flowing artesian wells. In the original USUGWM, transmissivity is linearized in a cycle by substituting a known head (HFC) in the former cycle for an unknown head (H) in the current cycle. However, the large number of nonsmooth functions describing q^e, q^d, q^f, and q^{rd} in the East Shore Area make it difficult to achieve feasible solutions for each cycle. When the linearized formulas of nonsmooth functions in the original USUGWM are used, the following problems occur:

1. The feasible solution is declared to be infeasible if initial guesses of head are far from the optimal heads.
2. If the problem is not infeasible, it takes many cycles to achieve the true optimal solution.
3. The model behaves as if multiple optimal solutions exist --some of which are significantly smaller in magnitude than others.

In the presented modified USUGWM, the formulas and solving procedure for nonsmooth functions are improved to address the above problems.

Comparison of the original and modified USUGWMs

The linearized formula and solving procedure of the original and modified USUGWM are compared below:

Linearized formula. For example, an original drain discharge equation is described as Eq. 7. In the model, discharge, i.e. groundwater pumping, is a positive value, and recharge is a negative value. Since q^d is external flow leaving from drains (discharge), q^d should be 0 for h < bottom elevation of drain. Otherwise, it should be positive (Fig. 7(a)).

In both the original and improved USUGWMs, the linear segment is selected based on head HFC^{n-1} known from the previous cycle. Drain discharge, q^d, is computed as

$$q^d_{l,i,j} = \Gamma^d_{l,i,j}(H^n_{l,i,j} - B^d_{l,i,j}) \quad \text{for } HFC^{n-1}_{l,i,j} > B^d_{l,i,j} \quad (11a)$$

$$= 0 \quad \text{for } HFC^{n-1}_{l,i,j} \le B^d_{l,i,j} \quad (11b)$$

where

HFC^{n-1} known head in the previous (n-1 th) cycle.

H^n unknown head in the current (n th) cycle.

As a result, q^d becomes either a simple linear equation or zero in each cycle. However, a major difference is in the bounds applied to H^n based on HFC^{n-1}. In the original USUGWM, the bounds limit H^n to the range (linear segment) it occurred in the former (n-1) cycle (Fig. 7(b)). In the modified

USUGWM, H^n is either a free variable if $HFC^{n-1} > H^d$ or equals zero if $HFC^{n-1} < H^d$ (Fig. 7(c)). This permits MINOS the freedom to solve. By the end of cycling, all head below the drain bottom correctly have q^d's of zero. How this difference affects the solution procedure is described below.

Solution procedure. Assume variable head cells containing drains in a discretized aquifer system. Initial heads are above the drain bottoms while some optimal heads are below the drain bottoms.

The original USUGWM: Since the initial guesses of head are above the drain bottoms (Figures 8(a) and 8(d)), both the original and the improved models use Eq. 11a in the first cycle. However, if the drain discharge is declared as a positive variable (bounded to be nonnegative), then the solved problem here can be infeasible in some cases. (Because this positive declaration is akin to trying to force $q^d > 0.0$ or h > drain bottom at every cell with a drain, it might be infeasible). If the solution is feasible, the original model forces some heads to be at the elevation bottom in the first cycle (Fig. 8(b)), and the optimal solution in this case is smaller than the true optimal solution. In the next cycle, the heads fall below the drain bottoms because Eq. 11b is used for computation (Fig. 8(c)). Thus if the initial guess of head is not far from the optimal solution, meaning that the model is not expected to face the infeasibility mentioned above, the model can reach the true optimal solution after cycling. However, whenever heads fall below the drain

bottoms, heads reach the drain bottoms first. Thus it takes many cycles to reach the true optimal solution.

The modified USUGWM: Drain discharge is allowed to be negative temporally during cycling, but it becomes either zero or a positive value as subsequent cycles converge. In the first cycle, some heads fall below the drain bottoms, and the drain discharge becomes negative (Fig. 8(e)). In this case, the optimal pumping is larger than the true optimal pumping because the model behaves as if recharge occurred from the drain. In the next cycle, q^d's are zero at these cells since Eq. 11b is used instead of Eq. 11a. Here, the negative values disappear (Fig. 8(f)). Thus the model can reach the true optimal solution faster without having the problems which occur in the original USUGWM.

RESPONSE MATRIX SIMULATION/OPTIMIZATION (S/O) MODEL

The principle of superposition cannot be used for unconfined aquifer systems without certain assumptions since the governing groundwater flow equation (Eq. 1) is nonlinear for such systems. Even if the aquifer system is confined or the saturated thickness is great enough that linearity can be assumed but if it contains significant external flows described by nonsmooth functions such as drain discharge, the assumption of linearity is also violated when head moves from one linear segment to another linear segment (Fig. 8(a)).

The basic idea for addressing these nonlinearities is the same as in the embedding model except that superposition

rather than embedding is used to compute heads. To satisfy the assumption of linearity through convergence and to permit the application of the response matrix (superposition) approach to nonlinear systems, the following approach is used.

Generating influence coefficients

The McDonald and Harbaugh (MODFLOW) model can be used as the Influence Coefficient Generator (ICG) for the linear system, even if the system is multilayered, because vertical flow terms, described as $CV(h_{l+1,i,j}-h_{l,i,j}) + CV(h_{l-1,i,j}-h_{l,i,j})$, are linear. However, this model cannot be used directly as the ICG for the nonlinear system.

In MODFLOW, the nonlinearities described above are solved using heads known from the former (m-1 th) iteration. Here, we use the Strong Implicit Procedure (SIP) for solving a large system of simultaneous linear equations by iteration.

Transmissivity of the unconfined aquifer is linearized by using heads ($HNEW^{m-1}$) known from the former (m-1 th) iteration to compute hydraulic conductances CR, CC for the current (m th) iteration. As a result, CR and CC are assumed constants. Similarly, any external flow consisting of two or three linear segments is linearized based on heads ($HNEW^{m-1}$) known from the former (m-1) iteration.

$$q^d_{l,i,j} = \Gamma^d_{l,i,j}(HNEW_{l,i,j}-B^d_{l,i,j}) \quad \text{for } HNEW^{m-1}_{l,i,j} > B^d_{l,i,j} \quad (12a)$$

$$= 0 \quad \text{for } HNEW^{m-1}_{l,i,j} < B^d_{l,i,j} \quad (12b)$$

where

HNEW unknown head in the current iteration

Therefore, q^d is described as either a simple linear equation or zero in each iteration. Then, SIP solves the linear equation (Eq. 3). Many iterations are usually required to converge to a solution.

Since we are using MODFLOW to generate influence coefficients, we must emulate the above process for compatibility between the management model and MODFLOW. A cycle in the development of influence coefficients and computation of the optimal strategy will be similar to the effect of a single iteration in MODFLOW. The approach is to use the same assumptions in developing influence coefficients and in computing the optimal strategy. Some of the assumed equation segments of Type 3 external flows will be wrong. However, they will be corrected by cycling just as MODFLOW assumes and corrects these equations by iteration.

Construction of the ICG required three actions: First, the McDonald and Harbaugh model is modified with respect to transmissivity in the upper, unconfined aquifer, drain discharge, evapotranspiration, discharge from flowing wells, and vertical flow reduction. The "Pre-ICG" is designed to perform the steady-state simulation through solving the flow equation (Eq. 3) repeatedly. This equation is linearized in each cycle by substituting head known from the former cycle rather than from the former iteration as described above.

Second, the simulation ability of the Pre-ICG is verified by comparing the simulation results with those of the MODFLOW including a flowing well subroutine.

Third, the Pre-ICG is designed to compute two kinds of steady-state influence coefficients.

h^{um}_o unmanaged head describing average steady-state head response over a cell only to known constant stresses (q^r: bedrock recharge, precipitation, etc. and these stresses do not include current nonoptimal pumping) (L^3/T);

$\delta_{o,m}$ influence coefficient describing the average head response over a cell only to a unit stress in a pumping cell m, (L^3/T).

Model formulation

In the response matrix S/O model, the same objective function and bounds on pumping are used as the embedding model. However, bounds on head are set only at necessary cells, and the following superposition expression is used as constraints to compute heads at those cells.

$$h_o = h^{um}_o + \sum_{m=1}^{M} \delta_{o,m}\, q_m \qquad (13)$$

where

h_o average potentiometric head in cell, (L);

q_m stress of pumping in a cell m, (L^3/T).

PRELIMINARY APPLICATION SCENARIO TO RESPONSE MATRIX S/O MODEL

Objectives of this section are (1) to demonstrate how required memory can be reduced using the response matrix approach for some scenarios and (2) to compare the applicability of the

embedding and response matrix models to the East Shore Area study. As shown in Table 2, both models are formulated to determine the maximum sustained yield from the 61 cells, which contain the existing M&I use pumping wells installed in the middle and lower layers. Flow charts in Fig. 9 compare the solution procedures. Both models are repeatedly optimized until variables do not change with the cycles. However, in the response matrix model, two external simulations (ICG and Pre-ICG) are involved in the cycle.

Bounds on variables

Bounds on pumping. The lower bound on pumping is the current withdrawal rate for all the existing pumping cells. For most cells, the upper bound on pumping is twice the current withdrawal rate. Exceptions are the 12 cells containing the Weber Basin W.C.D. and Hill A.F.B. wells. There, existing well capacities are the upper bounds on pumping.

Bounds on head in specific pumping cells. In the 12 cells containing the Weber Basin W.C.D. and Hill A.F.B. wells where large pumping has occurred, the maximum allowable drawdown is 20 ft below 1985 head.

Bounds on head of the unconfined aquifer. Heads in cells of the upper-shallow, unconfined aquifer are not allowed to fall below the base of the layer. In the embedding model, the bounds on head are easily set for all cells (1,270 cells) of the upper, unconfined aquifer since every cell contains the

flow equation. Thus there is no increase of required memory resulting from setting bounds on variables.

In the response matrix model, it is impractical to set the bounds on head for 1,270 cells. Sixty-one pumping cells x 1,270 cells = 77,470 influence coefficients would result in a huge memory allocation. For this preliminary testing, it is assumed that if head in the cell where the saturated thickness in 1985 is the thinnest does not fall below the base of the aquifer layer, then heads in any other cells will not fall below the geological bottom. Thus only one head located at layer 1, row 19, column 25 (1,19,25) is computed with 61 influence coefficients (δ) and unmanaged head (h^{um}) and is bounded in the management model. Post-optimization simulation verifies that no other cells are completely dewatered either (although undesirable drawdowns might occur).

Computation of head with Pre-ICG

Cycling requires estimating heads in an unconfined aquifer and in cells containing nonsmooth functions (for q^e, q^d, q^f, and q^{rd}) as input for the ICG in the next cycle. In this preliminary test, heads only in 13 cells are computed in the management model using Eq. 13. The Pre-ICG computes other heads in the current cycle using heads in the former (n-1 th) cycle and optimal pumping rates in the current (n th) cycle.

Results from embedding and response matrix S/O models

Heads in 1985 are used as the initial guesses. Optimal pumping rates and computed heads from both models are almost

identical. If more effort were made to identify a better combination of SIP parameters, the results between the models might be even closer. However, that would require more iterations of the ICG and more CPU time in generating influence coefficients. Table 3 compares computational resource required by both models. We used the VAX 5240. The response matrix model uses less than 6% of the memory required by the embedding model in every cycle. In terms of the required CPU time, the embedding model requires 103 minutes for the first cycle but only about 4 minutes after the second cycle. The response matrix model needs 8 to 13 minutes for every cycle, including running two external simulation models. Since both models need ten cycles to converge, total CPU time is slightly less for the response matrix model. However, if any new bounds or constraints require new influence coefficients generation, then the response matrix model could need more total CPU time than the embedding model.

Selection of S/O model for subsequent optimizations

In this study area, existing pumping wells are located at 61 cells. Most commonly, lower bounds on head are proposed at pumping cells. This assumes that the maximum drawdown occurs at a pumping cell. If this assumption is used for scenarios considering only the existing pumping as in this preliminary scenario, the response matrix model looks better than the embedding model because it uses less memory despite the need for regenerating influence coefficients for any changes of

bounds and constraints.

However, that approach might not be appropriate here. The maximum drawdown always occurs between wells near the mountains and the mountains in Layers 2 and 3 (Fig. 13). Furthermore, we cannot specify a location where the maximum drawdown might occur. Thus we propose tight lower bounds on head (maximum drawdown) in the entire city zone for subsequent management scenarios (discussed in the next section). In addition, we propose to permit pumping in many more cells. For this situation, the response matrix model is not practical. It would require too many simulations to generate influence coefficients. Also too many influence coefficients would be needed in constraint equations. This results because this is a steady-state optimization, and most of the concern is about heads in confined layers. Pumping in one lowest layer all affects steady heads at most other middle and lowest layer cells. Thus memory requirement would be huge for an optimization. In the embedding model, such bounds can be easily set using the same amount of memory as in the model without the bounds.

In conclusion, the response matrix model is a viable alternative to the embedding model for steady-state optimizations if constraints and bounds on variables do not need to be specified to many locations. At this stage of this study, it was difficult to specify how many potential pumping cells and head constraints would be needed. Because of its flexibility and easy adaptability, the embedding model was

selected for subsequent optimization.

USE OF EMBEDDING S/O MODEL FOR PERENNIAL-YIELD PUMPING STRATEGIES

The results of alternative future scenarios are compared. Due to the rapid urbanization in the area over the last 20 years, the demand for M&I water has increased markedly, but demand for irrigation water, which is mainly obtained from the Weber River, has not increased much. Those trends are expected to continue. Common assumptions for all scenarios are: (1) it is more important to extract water for M&I use than to have flowing wells for agricultural use, and (2) it is desirable that optimal pumping not be less than current pumping in any cell.

The study area is divided among the 25 water entities of Davis, Weber, and Box-Elder counties. These entities are a city or group thereof served by a single local public supplier or a wholesaler, Weber Basin W.C.D. (Fig. 10).

In overview, scenario 1 is the nonoptimal scenario. For the other scenarios, optimal sustainable annual groundwater pumping rates are computed using the modified version of the USUGWM. In scenario 2, the model maximizes the total sustainable pumping rate from the 61 cells containing wells currently pumping for M&I use. If existing wells cannot supply water of sufficient quantity and quality, one approach to meet the increasing water demand is to install new, large, pumping wells. The S/O model can help choose appropriate locations from many candidate pumping cells. In scenarios 3

and 4, this ability is demonstrated. Table 4 summarizes model formulations for the different scenarios. Figure 11 summarizes optimal water balance for these strategies.

Bounds on pumping and head for management scenarios

The following bounds on head and pumping are considered for all management scenarios:

Bounds on head. To avoid or minimize problems resulting from unacceptable drawdowns of the middle and lower layers where flowing and pumping wells are installed, the lower bounds on head of those layers are set as

$$h^{city}_{2,i,j} \leq h^{city}_{2,i,j} \text{ in } 1985 - D^L \quad (14a)$$

$$h^{city}_{3,i,j} \leq h^{city}_{3,i,j} \text{ in } 1985 - D^L \quad (14b)$$

where

h^{city} heads at cells within the city zones (= the water entity limits) as shown in Fig. 10.

D^L maximum acceptable cell drawdown.

The lower bound on head in Layer 1 is the aquifer bottom.

$$h_{1,i,j} > \text{Bottom}_{1,i,j} \quad (15)$$

Bounds on pumping. The lower bound on pumping is the current pumping rate for all existing wells. Upper bounds on pumping are usually based on well capacity or water requirements. In this model, for 12 cells containing Weber Basin W.C.D. and Hill A.F.B. wells, the well capacities are used as the upper bounds. These well capacities far exceed the current withdrawal rates. For other existing pumping wells, the upper bound is a multiple of the current pumping.

Scenario 1: nonoptimal scenario

The simulation option of the embedding method is used to predict the additional water-level declines that will ultimately result from continuing current withdrawals from flowing and pumping wells. It takes eight cycles for convergence (using 1985 heads as the initial guesses).

Scenario 2a: pumping from existing wells

In this scenario, the model maximizes total perennial-yield pumping in the 61 cells where pumping wells for M&I use currently exist. In most cells, except for the 12 cells that contain Weber Basin W.C.D and Hill A.F.B. wells, the upper bound on pumping is twice the current withdrawal rate. The maximum allowable drawdown in the entire city zone is 20 ft, so the lower bound on head is 20 ft below 1985 heads.

Computed steady-state water budgets. Total optimal pumping rate increases 50% to 48.4 cfs from current pumping (Fig. 11). The increase in pumping causes a decline of water levels in the upper unconfined aquifer and potentiometric heads in the middle and lower confined aquifer. This decline decreases the discharge from flowing wells and drains, upward inflow to the Great Salt Lake, and evapotranspiration. Their decreases in discharge are 25% and 12%, 6% and 3% of the nonoptimal discharge, respectively.

Spatial distribution of pumping and flowing discharge. In Davis county, pumping increases in all water entities except for South Weber and totals 14.6 cfs, which is 90% of

the regional pumping increase. On the other hand, in Weber county, pumping increases only 1.6 cfs in two water entities, which are West Weber and Roy. The total discharge of pumping and flowing wells decreases 3.3 cfs compared with the nonoptimal scenario. The decrease in flowing discharge is greatest in Syracuse, West Point, and West Weber.

Scenario 2b: effects by changing bounds on pumping and head

To analyze its effect on optimal pumping, the model is also run for different sets of lower and upper bounds on pumping and maximum allowable drawdown.

Upper bound on pumping. In most cells, except for those 12 cells that contain Weber Basin W.C.D. and Hill A.F.B. wells, the upper bound on pumping is varied: four, six, and ten times the current withdrawal rate. Other bounds are the same as in scenario 2a. In scenario 2a, the upper bound on pumping is twice the current pumping. By increasing the upper bound on pumping from twice to ten times the current pumping, the optimal sustainable pumping rate increases by 3.3 cfs to 51.7 cfs as shown in Table 5.

Lower bound on pumping. The lower bound on pumping is varied: 95%, 90%, and 80% of the current withdrawal rate for all existing pumping wells, while other bounds are the same as in scenario 2a. By releasing the lower bound on pumping from 100% of that in scenario 2a to 80% of the current pumping, the optimal sustainable pumping rate increases by 4.1 cfs to 52.5 cfs (Table 5).

Maximum allowable drawdown: The maximum allowable drawdown inside the city zone is varied: 15 ft, 25 ft, 30 ft, and 40 ft, while other bounds are the same as in scenario 2a. The problem is infeasible using 15 ft bound because heads near North Ogden fall below more than 15 ft simply to maintain the current pumping rate for all existing wells. When the lower bound on pumping is released to 70% of the current pumping rate for all existing cells, an optimal solution is found. In cases of 25 ft, 30 ft, and 40 ft, optimal sustainable pumping rates are 9.5 cfs, 13.1 cfs, and 19.4 cfs greater than that of scenario 2a, respectively (Table 5). The model is more sensitive to the increase of the maximum allowable drawdown than to the changes of the lower and upper bounds on pumping.

Scenario 2c: trade-off between pumping and flowing discharge

If pumping for M&I use increases in the urban area along the Wasatch Front mountains, then discharge from flowing wells on the agricultural lands will decrease. A conflict over water may occur between irrigation users and M&I users. There exists a tradeoff between pumping discharge for M&I use and flowing discharge for irrigation use. To consider the trade-off, the following constraint is added to the constraints of scenario 2a: Total discharge from the flowing wells for each water entity should meet or exceed a specified proportion of the discharge in the nonoptimal scenario.

$$\sum_{f=1}^{N^f} q^f \geq r \left[\sum_{f=1}^{N^f} unmanaged\ q^f\right] \qquad (16)$$

where

r parameter represents a fraction of total discharge of the nonoptimal scenario for each water entity.

q^f discharge from flowing wells in a cell, (L^3/T);

N^f total number of cells containing flowing wells for each water entity.

The model is run using various values of parameter (r). As the value of r decreases, the total optimal sustainable pumping rate increases, and the total discharge from the flowing wells decreases almost linearly (Fig. 12). This curve can be considered to be the pareto optimum between the objective of maximizing pumping and maximizing free flow from artesian wells.

Scenario 3a: pumping from proposed wells along irrigation conveyance system

If the results of implementing the strategy of scenario 2 are unsatisfactory, additional groundwater can be developed by installing new pumping wells along the existing water conveyance system. There are 17 main irrigation conveyance systems including that of the Weber Basin Project. Potential additional pumping cells exist in all water entities except for Centerville which includes none of the 17 irrigation conveyance systems. In this scenario, candidate sites for new pumping wells are located in 75 cells in the lower aquifer along the main irrigation conveyance systems. These sites are advantageous in having relatively high pressure for distributing water for M&I use (due to their

relatively higher elevations) and the ease with which pumping groundwater can be placed in the conveyance system. The objective function is to maximize total groundwater pumping from the existing and proposed wells (61+75=136 cells). Constraints and bounds on head and existing wells are the same as in scenario 2a--lower and upper bounds on pumping in new candidate cells are 0 and 1,000 gpm (1.114 cfs), respectively.

Computed steady-state water budgets. Total optimal pumping rate is 179% of the current pumping rate, while discharge from flowing wells, drain discharge, evapotranspiration, and upward inflow to the Great Salt Lake are 58%, 85%, 95%, and 90% of the nonoptimal rates, respectively (Fig. 11). Discharge from flowing wells ceased at 245 out of the original 813 flowing well cells (Table 6). The area, where flowing wells cease to flow, expands from the mountain side where potentiometric heads of the lower and middle layers are originally close to the ground surface (Fig. 2).

Spatial distribution of pumping and flowing discharge. Regional optimal pumping is 9.2 cfs greater than that of scenario 2a. There is discharge in 24 new pumping cells (Table 7). The spatial distribution of pumping differs from scenario 2a. The increase in pumping concentrates in Syracuse, West Point, and West Weber. There, the aquifer is not intensively developed and new pumping cells line the Layton canal. The net increase of total pumping and flowing

discharge is unequally distributed and increases in only five water entities (Table. 8).

Scenario 3b: assuring total discharge from wells

In this scenario, we assume that a reduction in water from flowing wells can be compensated for using water from newly installed pumping wells along the main canals in each water entity. While the objective function and bounds on head and pumping are the same as in scenario 3a, the following constraint is considered to address this scenario: Total supply of groundwater from either pumping wells or flowing wells for each water entity should meet or exceed that in the nonoptimal scenario (for all entities having current pumping or candidate pumping).

$$\sum_{i-1} (gp + q^f) \geq \sum_{i-1}^{N} nonoptimal\ (gp + q^f) \qquad (17)$$

Optimal sustainable groundwater pumping rate decreases 4.2 cfs from scenario 3a to 53.4 cfs, while flowing well discharge increases 2.4 cfs to 23.1 cfs. By assuring total discharge from both pumping and flowing wells, total discharge from wells for all water entities except for Centerville, in which no pumping cells exist, are more than zero as shown in Table 8. However, the spatial distribution of the increase in pumping is generally the same as in scenario 3a--concentrated in Syracuse, West Point, and West Weber.

Scenario 4a: pumping from proposed wells within water entities

In this scenario, an attempt is made to determine the potential for additional groundwater development at all cells of the lower layer inside city limits, with exception of the low development potential areas. The excluded areas are the low lands below 4,215 ft along the Great Salt Lake (lake level: 4,200 ft) and the area containing high TDS expanding from the east of Ogden to Plain City (Hansen Allen & Luce, Inc.[14]). We assume here that each water entity will have to develop the groundwater reservoir under its own area and meet its own water demand with groundwater as much as possible. The objective function is to maximize total groundwater pumping from the existing and proposed well sites (61+785=846 cells), while constraints and bounds on head and pumping wells are the same as in scenario 3a.

Drawdowns in 78 cells are 20 ft of the maximum drawdown. It is still impractical to use the response matrix model even if the tight bounds on head could be specified only for these cells. A huge memory allocation of 846 potential pumping cells x 78 cells = 65,988 influence coefficients would result. Furthermore, the ICG must rerun 846 times to generate influence coefficients for unit pumping.

Computed steady-state water budgets. Total optimal pumping rate increases to 205% of the current pumping rate while discharge from flowing wells, drain, evapotranspiration, upward inflow to the Great Salt Lake from the underlying aquifer decreases to 47%, 79%, 94%, and 82% of the nonoptimal

rate, respectively (Fig. 11). Intrusion of salt water from the Great Salt Lake at 24 cells totals 0.052 cfs. Discharge to the lake at another 425 cells totals 17.7 cfs. No downward inflow from the Great Salt Lake is recognized in the other scenarios (except for scenario 2b2 and 2b3, in which downward inflow totals 0.003 cfs).

Spatial distribution of pumping and flowing discharge. The pumping increase is mostly concentrated in newly proposed pumping cells. Of the 785 newly proposed pumping cells, the model choose to pump at 81 cells. These are distributed in the northwestern part of West Weber and along the shore of the Great Salt Lake in Davis county, such as in Syracuse, West Point, Kaysville, Farmington, and Centerville (Table 7).

Scenario 4b: preventing salt water intrusion

To prevent the intrusion of salt water from the Great Salt Lake, the following bound in all cells with general head boundary is added to the constraints in scenario 4a.

$$q^g_{1,i,j} \geq 0.0 \qquad (18)$$

The resulting tradeoff to prevent any lake water downflow to the aquifer is a 1.7 cfs decrease in regional pumping (Fig. 11). The spatial distribution of new pumping wells in West Weber differs from that of scenario 4a. The number of new pumping cells in West Weber decreases from 29 cells to 14 cells (Table 7). Thus there are 127 cells with nonzero pumping (61 existing and 66 new proposed pumping cells).

Scenario 4c: egalitarian goal

The total pumping of 67.9 cfs in scenario 4a indicates the physical development potential from the entire aquifer for the specified bounds on head and pumping. However, the pumping increases in only prespecified areas. Further changing the bounds on pumping and head will not permit much more regional change even if different sets of bounds on pumping and head are used for this scenario. Such a strategy cannot be adopted for economic and egalitarian reasons. In this scenario, an attempt to develop a more egalitarian pumping strategy is performed. If future excess in groundwater extractions is allocated to water entities in proportion to their area and the withdrawal must occur within their boundaries, then less sustainable pumping is possible.

This is accomplished by setting the following objective function and constraints; other constraints are the same as in scenario 4a. The objective function is to maximize a ratio (r) of increased pumping to an assumed upper limit on pumping.

$$\textit{maximize } r \tag{19}$$

For each water entity, the ratio (rw) is constrained:

$$rw = \frac{AD}{ULDP} \tag{20}$$

where

AD = additional development (optimal-current) pumping

ULDP= upper limit of development potential pumping

= areal size ratio of each water entity to the whole water entity limits x maximum additional sustained yield of the whole water entity limits

This ratio (rw) should be the same for all water entities based on the egalitarian goal.

$$r = rw \tag{21}$$

The maximum additional total sustained yield is 33.7 cfs since total perennial-yield in scenario 4a is 65.9 cfs and the total of the current pumping rates is 32.2 cfs. Table 9 shows area, areal ratio, ULDP, and optimal additional development of pumping (AD) across water entities. The optimal ratio is 0.28. The ratio is low because withdrawal from all water entities of Weber county, except for West Weber, is restricted due to their drawdowns. If the maximum allowable drawdown for these areas can be relaxed, the ratio will be improved significantly.

Vertical water movement between layers

On the agricultural lands near the Great Salt Lake, the water table of the shallow and unconfined aquifer is lower than heads of the underlying layers allowing water to move upward through leakage (Fig. 2). In this condition, groundwater contaminants--pesticides and insecticides--remain in the shallow aquifer. However, the downward movement of low-quality groundwater of the shallow aquifer to the confined aquifer may occur by the large-scale withdrawal from the underlying confined aquifers.

Table 10 summarizes upward and downward movement of water between the upper and middle layers (Layers 1 & 2) and between the middle and lower layers (Layers 2 & 3). As additional groundwater development increases, downward flow from the middle layer to the lower layer increases significantly. In scenario 4a, which is the most developed case, the downward flow occurs in 227 cells of the 1,644 cells and totals 5.593 cfs. On the other hand, the downward movement from the upper layer to the middle layer--the deterioration of water quality being the main concern--is not significant. In scenario 4a, the downward movement occurs only in 10 cells and totals only 0.082 cfs. As long as additional groundwater is pumped primarily from the lowest layer, significant downward flow from the uppermost layer will not occur. However, the model does not consider a seasonal fluctuation of head such as extreme drawdowns resulting from pumping in the summer. This may cause intrusion or low quality water from the upper shallow aquifer. Therefore, a more detailed investigation of groundwater water quality problems is appropriate for setting bounds on head.

Conclusion for these tested scenarios is that there is not much chance of contaminants moving downwards to lower levels. However, contaminants can enter the major aquifer where they are unconfined near the mountains.

Declines of potentiometric heads in the lower layer

For all scenarios, the decline of potentiometric heads exceeds 50 ft near North Ogden (outside of the city zone). For the nonoptimal case (scenario 1), no significant decline of heads occurs in the pumping center in the vicinity of the Hill A.F.B. (Fig. 13). For the optimal management scenarios, two typical patterns in decline of heads are found. One results from maximizing pumping from the existing pumping wells (scenario 2). The other results from maximizing pumping from the existing and/or newly proposed wells (scenarios 3 and 4). Figures 14 and 15 show the drawdown contours for scenario 2b (maximum allowable drawdown = 30 ft) and scenario 4b (maximum allowable drawdown = 20 ft), respectively. In both scenarios, optimal pumping rates are about twice the current pumping rate. In the vicinity of the Hill A.F.B., for scenario 2b, the declines of head are 25 ft to 30 ft. On the other hand, for scenario 4b, the declines are only 5 to 10 ft.

Validation of optimal solutions

Steady-state flow simulation. The flow simulation ability of the S/O model is confirmed by comparing optimal heads with heads simulated to results from optimal pumping values. Heads were simulated using a McDonald and Harbaugh model in which a flowing well subroutine is added. Optimal pumping rates from scenarios 1, 2a, 3a, and 4a are used as input data for this comparison. Both models estimate almost identical heads, discharge from flowing wells and drains,

evapotranspiration, and general-head boundary interflow. The absolute value of the maximum difference between simulated heads obtained from the two models does not exceed 0.02 feet in any cell.

Evolution of head to the optimal steady-state. To trace the evolution of heads to the optimal steady-state, transient 50-year simulations using optimal pumping strategies for the above scenarios are performed. The McDonald and Harbaugh model is run to get transient solutions for five 10-year stress periods in which each stress period is divided into four time steps. Heads in 1985 calibrated by USGS are used as initial heads. At each time step, total absolute differences (TAD) between transient heads and optimal steady-state heads are calculated and plotted as shown in Fig. 16. The time required to achieve the optimal steady-state heads depends on how far an initial head is from an optimal solution. If we assume that heads reach the optimal steady-state when TAD attains 200 ft (average difference between optimal head and attained head of of 200 ft for 4,880 cells = 0.04 ft), then the head evolution era are 11, 20, 30, and 40 years in duration for scenarios 1, 2a, 3a, and 4a, respectively.

Global optimality. Since the problems are highly complex and nonlinear, it is necessary to confirm global optimality of solutions (even though global optimality of the LP solution to the linear surrogate problem is guaranteed). By allowing variables such as evapotranspiration, drain discharge, and flowing wells to be negative in each cycle, the model can

converge to the stable solution even if the initial guess is far from the optimal solution. Therefore, we assume here that the global optimality is guaranteed if the optimal solution does not increase by changing the starting point--an initial guess of the optimal solution which is either close to or far from the optimal solution. For confirmation, the model is run for scenario 2a using different sets of the initial guess, in which the furthest one is a set of variables including heads in 1985 and the closest one is scenario 2b having four times the current pumping as the upper bound. In all cases, optimal solutions vary by no more than 0.01% from each other. In conclusion, the optimal solution computed by the S/O model can be considered to be very close to the global optimal. How close one gets depends on the convergence criterion used for stopping cycling.

SUMMARY AND CONCLUSIONS

The development and use of a cycling procedure for applying embedding and response matrix approaches to an extremely large, complex, nonlinear/linear aquifer system are presented and tested. The addressed groundwater reservoir in the East Shore Area of Utah is discretized into 4,880 finite-difference cells in the model. The cycling procedure involves repeating the optimization of linearized forms of nonlinear flow equations to reach the true optimal solution. The solved problem is large and nonlinear since the upper, unconfined (nonlinear) aquifer is discretized into 1,274 cells. Also

involved are 2,123 nonsmooth functions describing discharge from flowing wells, drain discharge, and evapotranspiration. To facilitate both approaches for this aquifer system, new developments include:

A. The linear version of USUGWM is improved by completely linearizing nonsmooth functions. The model uses the embedding approach and treats transmissivity and nonsmooth functions linearly in each cycle. This improvement enables the USUGWM to converge to a stable optimal solution in any initial guess in a wide range. The modified version of the USUGWM has around 40,000 nonzero elements, 12,000 single equations and variables. The previously reported disadvantage of the embedding model is mainly computational difficulty resulting from its large dimensionality. This study shows that the embedding model can solve such a huge nonlinear system.

B. To correctly represent the above nonlinear system while satisfying the principle of superposition, the response matrix model uses cycling and linear influence coefficients generated using a modified McDonald and Harbaugh (MODFLOW) model. In the modified MODFLOW, the above nonlinear system is treated linearly in each cycle. The linear segments of nonsmooth functions are selected based on head known from the previous cycle. Some of the selected linear segments of the nonsmooth functions are wrong. However, they will be corrected through cycling just as MODFLOW corrects equation assumptions through

iteration. In the management model, only heads of interest are computed using superposition. After optimization, the modified MODFLOW computes other heads, which are necessary to implement the next cycle (to select the linear segments of nonsmooth functions and to compute transmissivity in an unconfined aquifer). This model is the first response matrix S/O model which has the same steady-state simulation abilities of MODFLOW.

After comparison between the response matrix and embedding S/O models for a preliminary scenario, the embedding model is selected for further use. Selection is based on its ability to address large numbers and potential pumping cells.

Four groups of scenarios are tested. All management scenarios consider pumping from 61 existing pumping cells and/or many other potential pumping cells. Some scenarios constrain discharge from flowing wells at 813 cells. The embedding model, a modified version of the USUGWM, can compute the perennial-yield pumping rate for the presented scenarios.

The general conclusions for the tested scenarios are as follows:

1. The groundwater reservoir can be developed physically to meet the increasing demand of water for M&I use in the East Shore Area. In the tested scenarios, the largest sustainable pumping yield is 205% of the current pumping. However, the additional development potential relies heavily on groundwater underlying agricultural lands near the lakeshore. There, much groundwater currently

discharges by itself through flowing artesian wells.

2. An increase of pumping for M&I use will almost linearly decrease the discharge from flowing wells for irrigation use.
3. For computed pumping strategies that allow to develop groundwater in the lowest aquifer, a large amount of low quality water in the upper, shallow aquifer will not intrude into the fresh water in the underlying confined aquifers.
4. In this model, a uniform maximum allowable drawdown is used for the entire study area. More pumping could be obtained by permitting more drawdown in some locations. However, determining what is acceptable requires detailed analysis beyond the scope of this study.

The models presented here are useful for reconnaissance-level perennial-yield planning of a large, complex, unconfined/confined aquifer system. For this purpose, the embedding model is preferred because of its flexibility in changing sets of bounds and constraints, numbers of pumping cells, and its ability to handle numerous external flows. This flexibility permits planners to readily consider pumping and drawdown consequences in many locations and to change locations of interest. This is helpful to planners who cannot easily a priori specify all which might result from development and the locations where these problems might occur. On the other hand, the response matrix model is a valuable alternative. It can require less memory if the

number (proportion) of pumping cells and cells requiring head constraint are not large.

REFERENCES

1 Aguado, E. and Remson I. Ground-water hydraulics in aquifer management. *Journal of Hydraulic Division, American Society of Civil Engineers*, 1974, 100(HY1), 103-118

2 American Society of Civil Engineers. Ground water management, ASCE Manuals and Reports on Engineering Practice No. 40, American Society of Civil Engineers, New York, New York. 1987

3 Bear, J. Hydraulics of groundwater. McGraw-Hill, New York. 1979

4 Brooke, A., Kendrick, D., and Meeraus, A. GAMS: A user's guide, The Scientific Press, Redwood, California. 1988

5 Bolke, K. L. and Waddle, K. M. Groundwater conditions in the East Shore Area, Box Elder, Davis, and Weber counties, Utah, 1960-1969, Technical Publication No. 35, State of Utah, Department of Natural Resources, Salt Lake City, Utah, 1972

6 Cantiller, R. R. A., Peralta, R. C. and Azarmnia, H. Optimal conjunctive use-sustained yield pumping analysis for eastern Arkansas, Miscellaneous Publication No. 40, University of Arkansas, Arkansas Water Resources Research Center, Fayetteville, Arkansas, 1988

7 Clark, D. W., Appel, C. L., Lambert, P. W. and Puryear R. L. Groundwater resources and simulated effects of withdrawals in the East Shore Area of Great Salt Lake, Utah. Technical Publication No. 93, State of Utah and United States Geological Survey, Salt Lake City, Utah, 1990

8 Danskin W. R. and Gorelick S. M. A policy evaluation tool: management of a multiaquifer system using controlled stream recharge. *Water Resour. Res.*, 1985, 21(11), 1731-1747

9 Eisele H., Etheshami M., Peralta, R. C., Deer H. M. and Tindall, T. Agricultural pesticide hazard to groundwater in Utah, Part I: Main Report, Report of the Department of Agricultural and Irrigation Engineering and Extension Service, Utah State University, April 1989

10 Elwell, B. O. and Lall, U. Determination of an optimal aquifer yield, with Salt Lake County applications, *J. of Hydrology*, 1988, 104, 273-278

Gharbi, A, Peralta, R. C. and Waddell, K. M. odelling for potentiometric surface management of ltilayer aquifer systems, International Summer ting, Columbus, Ohio, American Society of cultural Engineers, 1990, Paper No. 90-2060

12 Gharbi, A. Optimal groundwater quality and quantity management with application to the Salt Lake Valley. Unpublished dissertation of doctor of philosophy, Department of Agricultural and Irrigation Engineering, 1991

13 Gorelick, S. M. A review of distributed parameters groundwater management modeling method, *Water Resour. Res.*, 1983, 19(2), 305-319

14 Hansen Allen & Luce Inc. Personal communication and a report to the Civil Engineering Department (Water Resources Division), Utah State Univ., 1990

15 Heidari, M. Application of linear system's theory and linear programming to groundwater management in Kansas, *Water Resources Bulletin*, 1982, 18(6), 1003-1013

16 Illangasekare, T. H., Morel-Seytoux, H. J. and Verdin, K. L. A technique of reinitialization for efficient simulation of large aquifers using the discrete kernel approach, *Water Resour. Res.*, 1984, 20(11), 1733-1742

17 Illangasekare, T. H. and Morel-Seytoux, H. J. Application of a physically-based distributed parameter model for arid-zone, surface-groundwater management, *J. of Hydrology*, 1984, 74, 233-257

18 Jones, L. C., Wiilis, R. and Yeh W. W. Optimal control of nonlinear groundwater hydraulics using differential dynamic programming. *Water Resour. Res.*, 1987, 23(11), 2097-2106

19 Knapp, K. C. and Feinerman, E. The optimal steady-state in groundwater management, *Water Resources Bulletin*, 1985, 21(6), 967-975

20 Maddock III, T. Algebraic technological function from a simulation model, *Water Resour. Res.*, 1972, 8(1), 129-134

21 Maddock III, T. Nonlinear technological functions for aquifers whose transmissivities vary with drawdown, *Water Resour. Res.*, 1974, 10(4), 877-881

22 McDonald, M. G. and Harbaugh, A. W. A three-dimensional finite-difference groundwater model, U.S. Geological Survey, Open File Report 83-875, 1988

23 Murtagh, B. A. and Saunders, M. A. MINOS 5.1 User's Guide, Report SOL 83-20R. December 1983, revised January 1987, Stanford University

24 Morel-Seytoux, H. J. and Daly, C. J. A discrete kernel generator for stream aquifer studies, *Water Resour. Res.*, 1975, 11(4), 253-260

25 Peralta, R. C. and Killian, P. J. Optimal regional potentiometric surface design: Least-cost water supply/sustained groundwater yield, *Transaction. American Society of Agricultural Engineers*, 1985, 28(4), 1098-1107

26 Peralta, R. C., Azarmnia, H. and Takahashi, S. Embedding and response matrix techniques for maximizing steady-state ground-water extraction: computational comparison, *Ground Water*, 1991, 29(3), 357-364

27 Price D. Ground water in Utah's densely populated Wasatch Front area - The challenge and the choices, USGS Water-Supply paper 2232. United States Geological Survey, Salt Lake City, Utah, 1982

28 State of Utah, Department of Natural Resources, Division of Water Rights. Water use data for public water suppliers in Utah, 1981, State of Utah, Department of Natural Resources, Division of Water Rights, Salt Lake City, Utah, 1982

29 State of Utah, Department of Natural Resources, Division of Water Rights. Water use data for public water suppliers in Utah, 1984 and 1985, State of Utah, Department of Natural Resources, Division of Water Rights, Salt Lake City, Utah, 1988

30 The United States Bureau of Reclamation, Weber Basin Water Conservancy Districts. Change of water use in Willard Reservoir, The United States Bureau of Reclamation and Weber Basin Water Conservancy Districts, Salt Lake City, Utah, 1987

31 Tung, Y. K. Groundwater management by chance-constrained model, *Journal of Water Resources Planning and Management*, 1986, 112(1), 125-136

32 Tung, Y. K. and Kolterman, C. E. Some computational experience using embedding technique for ground-water management, *Ground Water*, 1985, 23(4), 455-464

33 Yazdanian, A. and Peralta, R. C. Maintaining target groundwater levels using goal-programming: linear and quadratic methods, *Transactions. American Society of Agricultural Engineers*, 1986b, 29(6), 1696-1703

34 Venetis, C. Finite aquifer: characteristics, responses and application, *J. of Hydrology*, 1970, 12(3), 53-62

35 Willis, R. and Yeh, W. W-G.. Groundwater systems planning and management, Prentice-Hall, Inc., Englewood Cliffs, New Jersey, 1987

Shu Takahashi has earned a B.S. degree in Agricultural Engineering and a M.S. degree in Environmental Science from Hokkaido University, Japan. He has worked on irrigation development projects in developing countries. He is currently an engineer for Nippon Koei Co. Ltd. and a doctoral candidate in the Department of Biological and Irrigation Engineering at Utah State University.

Richard C. Peralta, P.E., holds a B.S, major in Chemistry, from the University of South Carolina, an M.S. in Agricultural and Irrigation Engineering from Utah State University, and Ph.D. in Agricultural Engineering (Water Resources) from Oklahoma State University. For 11 years he has been conducting ground-water management studies and developing models for irrigated areas.

Table 1. Number of finite-difference cells

Type of cells	Layer 1 (Upper)	Layer 2 (Middle)	Layer 3 (Lower)	Total
Active cells	1274	1644	1962	4880
Cells with pumping wells	0	10	51	61
Cells with flowing wells	0	402	411	813
Cells with ET[a]	708	0	0	708
Cells with drain	602	0	0	602
Cells with GHB[b]	449	0	0	449

[a]ET means evapotranspiration
[b]GHB means general head boundary

Table 2. Comparison of model formulation: the embedding and response matrix approaches for preliminary problem

	Components	Equation and or definition: Embedding	Equation and or definition: Response Matrix
A.	External simulation model		
1.	Pre-ICG	-	Yes
2.	ICG	-	yes
B.	Management model		
1.	Objective function	2(LP)	2(LP)
2.	Constraints		
	Flow equation	3(LP)	-
	Flowing wells	4(LP)	-
	General head boundary	5(LP)	-
	Evapotranspiration	6(LP)	-
	Drain discharge	7(LP)	-
	Vertical flow reduction	8(LP)	-
	Head computation	-	13(LP)
3.	Bounds		
	Heads		
	Layer 1	$H_{1,i,j} \geq Bot_{1,i,j}$	$H_{1,19,25} \geq Bot_{1,i,j}$
	at 12 WBWCD & Hill AFB		$H_{1,i,j} \geq H'^{85}_{1,i,j} - 20$ ft
	Pumping		
	12 WBWCD & Hill AFB wells		$gp^c \leq gp \leq gp^{cap}$
	Other existing wells		$gp^c \leq gp \leq 2 \times gp^c$
4.	Variable declaration		
	Positive	gp	gp
	Default (free)	$h, q^d, q^g, q^f, q^e, q^{rd}$	h
	Free	objective value	objective value
5.	MINOS solver	LP	LP
6.	Cyclic Procedure	Yes	Yes

gp^c means current pumping rate
gp^{cap} means well capacity

Table 3. Computational requirements of the embedding and response matrix models for preliminary problem

Items	Embedding	Response Matrix
Equations	12433	14
Variables	12521	102
Nonzero elements	46565	895
Required Memory (Mbytes)	7.04	0.4
CPU time		
1st cycle	103 min.	8 min.
after 1st cycle	about 4 min.	8 to 13 min.

Table 4. Summary of model formulations for various scenarios

Components/scenarios	Equation/definition						
	2a	2c	3a	3b	4a	4b	4c
1. Objective function							
Maximizing total gp	2	2	2	2	2	2	-
Egalitarian goal	-	-	-	-	-	-	19
2. Constraints							
Flow equation	3	3	3	3	3	3	3
Flowing wells	4	4	4	4	4	4	4
General head boundary	5	5	5	5	5	5	5
Evapotranspiration	6	6	6	6	6	6	6
Drain discharge	7	7	7	7	7	7	7
Vertical flow reduction	8	8	8	8	8	8	8
Tradeoff between gp&qf	-	16	-	-	-	-	-
Assuring net withdrawal	-	-	-	17	-	-	-
Excess/potential	-	-	-	-	-	-	20&21
3. Bounds							
Prevent salt water	-	-	-	-	-	18	-
Heads							
Layer 1	$H_{1,i,j} \geq Bot_{1,i,j}$						
Layer 2	$H^{city}_{2,i,j} \geq H'^{85}_{2,i,j} - 20$ ft						
Layer 3	$H^{city}_{3,i,j} \geq H'^{85}_{3,i,j} - 20$ ft						
Pumping							
Number of Existing & candidate locations	61	61	136	136	846	846	846
Bounds							
12 WBWCD & Hill AFB wells	$gp^c \leq gp \leq gp^{cap}$						
Other existing wells	$gp^c \leq gp \leq 2 \times gp$						
Newly proposed wells	$0 \leq gp \leq 1{,}000$ gpm						
4. Variable declaration							
Positive	gp						
Default (free)	$h, q^d, q^g, q^f, q^c, q^{rd}$						
Free	obj						
5. MINOS solver	LP						
6. Cycling procedure	YES						

Table 5. Computed water budgets for Scenario 2b's

(a) Total optimal pumping (cfs)

	Multiple of current pumping	1	2	gp^U 4	6	10
	1	32.21	48.40	49.98	51.26	51.75
gp^L	0.95	-	50.67	-	-	-
	0.90	-	51.74	-	-	-
	0.80	-	52.49	-	-	-
	Drawdown (ft)					
	20	-	48.40	-	-	-
D^L	30	-	57.92	-	-	-
	35	-	61.54	-	-	-
	40	-	67.82	-	-	-

(2) Total discharge from flowing wells (cfs)

	Multiple of current pumping	1	2	gp^U 4	6	10
	1	35.95	27.13	26.33	25.41	25.05
gp^L	0.95	-	26.03	-	-	-
	0.90	-	25.47	-	-	-
	0.80	-	25.12	-	-	-
	Drawdown (ft)					
	20	35.95	27.13	-	-	-
D^L	30	-	22.29	-	-	-
	35	-	20.71	-	-	-
	40	-	18.23	-	-	-

(3) Total of other discharge (Et, drain, and GHB) (cfs)

	Multiple of current pumping	1	2	gp^U 4	6	10
	1	80.23	72.86	72.08	71.72	71.59
gp^L	0.95	-	71.69	-	-	-
	0.90	-	71.18	-	-	-
	0.80	-	70.78	-	-	-
	Drawdown (ft)					
	20	-	72.86	-	-	-
D^L	30	-	68.18	-	-	-
	35	-	66.14	-	-	-
	40	-	62.34	-	-	-

gp^U is a upper bound on pumping, multiple of current pumping.
gp^L is a lower bound on pumping, multiple of current pumping.
D^L is a maximum allowable drawdown under 1985 head.

Table 6. Change in flow of flowing wells

Flowing condition	Number of cells			
	Scenarios			
	1	2a	3a	4a
Decrease or Cease	436	705	705	792
Cease	143	188	245	311
Increase	377	108	108	21
No change	0	0	0	0
Total	813	813	813	813

Table 7. Spatial distribution of existing and additional pumping cells across the water entities

Water entities	Number of cells with existing pumping wells	Number of cells with additional pumping wells				
		Scenarios				
		3a	3b	4a	4b	4c
Davis County	26	18	19	52	52	11
Centerville	0	0	0	2	0	1
Clearfield	3	0	0	0	0	1
Clinton	1	0	0	0	1	1
Farmington	3	1	1	14	13	1
Fruit Heights	1	2	3	0	0	1
Hill Field	6	0	0	0	0	0
Kaysville	0	0	1	14	15	1
Layton	4	0	1	1	2	1
So. Weber	3	0	0	0	0	1
Sunset	1	0	0	0	0	1
Syracuse	2	7	6	14	14	1
West Point	2	8	5	7	8	1
Weber County	31	6	9	29	14	11
Ogden	3	0	0	0	0	1
No. Ogden	8	0	0	0	0	0
Pleasant View	2	0	1	0	0	1
Harrisville	0	0	1	0	0	1
Farr West	2	0	1	0	0	1
Plain City	0	0	1	0	0	1
So. Ogden	2	0	0	0	0	1
Riverdale	4	0	0	0	0	1
Roy	1	0	0	0	0	1
Washington T	2	0	0	0	0	1
Uintah	0	0	0	0	0	1
West Weber	7	6	5	29	14	2
Box Elder County	4	0	1	0	0	1
Willard City	4	0	1	0	0	1
Total	61	24	26	81	66	23

Table 8. Pumping and Flowing Well Discharge for Water Entities for Scenarios 3a and 3b

Water entities	Scenario 3a			Scenario 3b		
	Δgp (cfs)	Δq^f (cfs)	Δtotal (cfs)	Δgp (cfs)	Δq^f (cfs)	Δtotal (cfs)
Davis County	15.725	-6.183	9.542	14.353	-5.737	8.616
Centerville	-	-0.042	-0.042	-	-0.042	-0.042
Clearfield	0.000	-	0.000	0.000	-	0.000
Clinton	0.000	-	0.000	0.000	-	0.000
Farmington	1.309	-0.397	0.912	1.277	-0.396	0.881
Fruit Heights	0.965	-	0.965	0.977	-	0.977
Hill Field	0.000	-	0.000	0.000	-	0.000
Kaysville	0.000	-0.176	-0.176	0.169	-0.169	0.000
Layton	0.000	-0.398	-0.398	0.389	-0.389	0.000
So. Weber	0.000	-	0.000	0.000	-	0.000
Sunset	0.000	-	0.000	0.000	-	0.000
Syracuse	6.717	-3.002	3.715	6.442	-2.814	3.628
West Point	6.734	-2.168	4.566	5.099	-1.927	3.172
Weber County	9.643	-8.714	0.929	6.803	-6.803	0.000
Ogden	0.000	-0.047	-0.047	0.041	-0.041	0.000
No. Ogden	0.000	-0.050	-0.050	0.053	-0.053	0.000
Pleasant View	0.000	-0.048	-0.048	0.063	-0.063	0.000
Harrisville	0.000	-0.092	-0.092	0.098	-0.098	0.000
Farr West	0.000	-0.140	-0.140	0.154	-0.154	0.000
Plain City	0.000	-0.196	-0.196	0.173	-0.173	0.000
So. Ogden	0.000	-	0.000	0.000	-	0.000
Riverdale	0.000	-	0.000	0.000	-	0.000
Roy	0.000	-	0.000	0.000	-	0.000
Washington T	0.000	-	0.000	0.000	-	0.000
Uintah	0.000	-	-	0.000	-	0.000
West Weber	9.643	-8.141	1.502	6.220	-6.220	0.000
Box Elder County	0.000	-0.008	-0.008	0.011	-0.011	0.000
Willard City	0.000	-0.008	-0.008	0.011	-0.011	0.000
Out of city zone	-	-0.268	-0.268	-	-0.245	-0.245
Total	25.368	-15.173	10.195	21.885	-13.182	8.728

Δ means change in discharge (increase or decrease) from discharge of the nonoptimal scenario to optimal discharge in the management scenario.

Table 9. Additional development of pumping under the egalitarian goal: scenario 4c

Water entities	Area (mile^2)	Aerial ratio (cfs)	ULDP (cfs)	Pumping SC1[a] (cfs)	SC4C[b] (cfs)	AD (cfs)
Davis County	98.875	0.415	13.968	22.627	26.540	3.913
Centerville	2.625	0.012	0.391	-	0.110	0.110
Clearfield	7.500	0.033	1.116	0.246	0.559	0.313
Clinton	5.750	0.025	0.856	0.017	0.257	0.240
Farmington	8.625	0.038	1.283	0.686	1.045	0.359
Fruit Heights	3.000	0.013	0.446	0.035	0.160	0.125
Hill Field	9.750	0.043	1.451	6.248	6.655	0.407
Kaysville	10.000	0.044	1.488	-	0.417	0.417
Layton	25.750	0.114	3.831	3.456	4.529	1.073
So. Weber	5.500	0.024	0.818	11.603	11.832	0.229
Sunset	1.000	0.004	0.149	0.067	0.109	0.042
Syracuse	11.750	0.052	1.748	0.175	0.665	0.490
West Point	2.625	0.012	0.391	0.094	0.204	0.110
Weber County	118.500	0.523	17.632	9.271	14.251	4.980
Ogden	22.750	0.100	3.385	0.043	0.991	0.948
No. Ogden	3.750	0.017	0.558	0.976	1.132	0.156
Pleasant View	7.750	0.034	1.153	0.200	0.503	0.303
Harrisville	4.000	0.018	0.595	-	0.107	0.107
Farr West	4.250	0.019	0.632	0.051	0.228	0.177
Plain City	4.000	0.018	0.595	-	0.167	0.167
So. Ogden	5.750	0.025	0.856	0.595	0.835	0.240
Riverdale	4.000	0.018	0.595	4.298	4.465	0.167
Roy	7.000	0.031	1.042	0.835	1.127	0.292
Washington T	2.000	0.009	0.298	0.775	0.858	0.083
Uintah	1.500	0.007	0.223	-	0.062	0.062
West Weber	51.750	0.229	7.700	1.498	3.655	2.157
Box Elder County	14.000	0.062	2.809	0.309	0.893	0.584
Willard City	14.000	2.500	2.809	0.309	0.893	0.584
Total	226.375	1.000	33.683	32.207	41.644	9.437

[a]SC1 means scenario 1
[b]SC4C means scenario 4c

Table 10. Vertical water movements

Item	Scenarios 1	2a	3a	4a
Layer 1 & 2				
Upward				
volume (cfs)	80.263	72.939	70.122	65.556
number of cells	1273	1268	1268	1264
Dounward				
volume	0.027	0.071	0.081	0.082
number of cells	1	6	6	10
Layer 2 & 3				
Upward				
volume (cfs)	83.001	73.383	69.280	64.664
number of cells	1603	1570	1534	1417
Downward				
volume (cfs)	1.676	2.321	2.398	5.593
number of cells	41	74	110	227

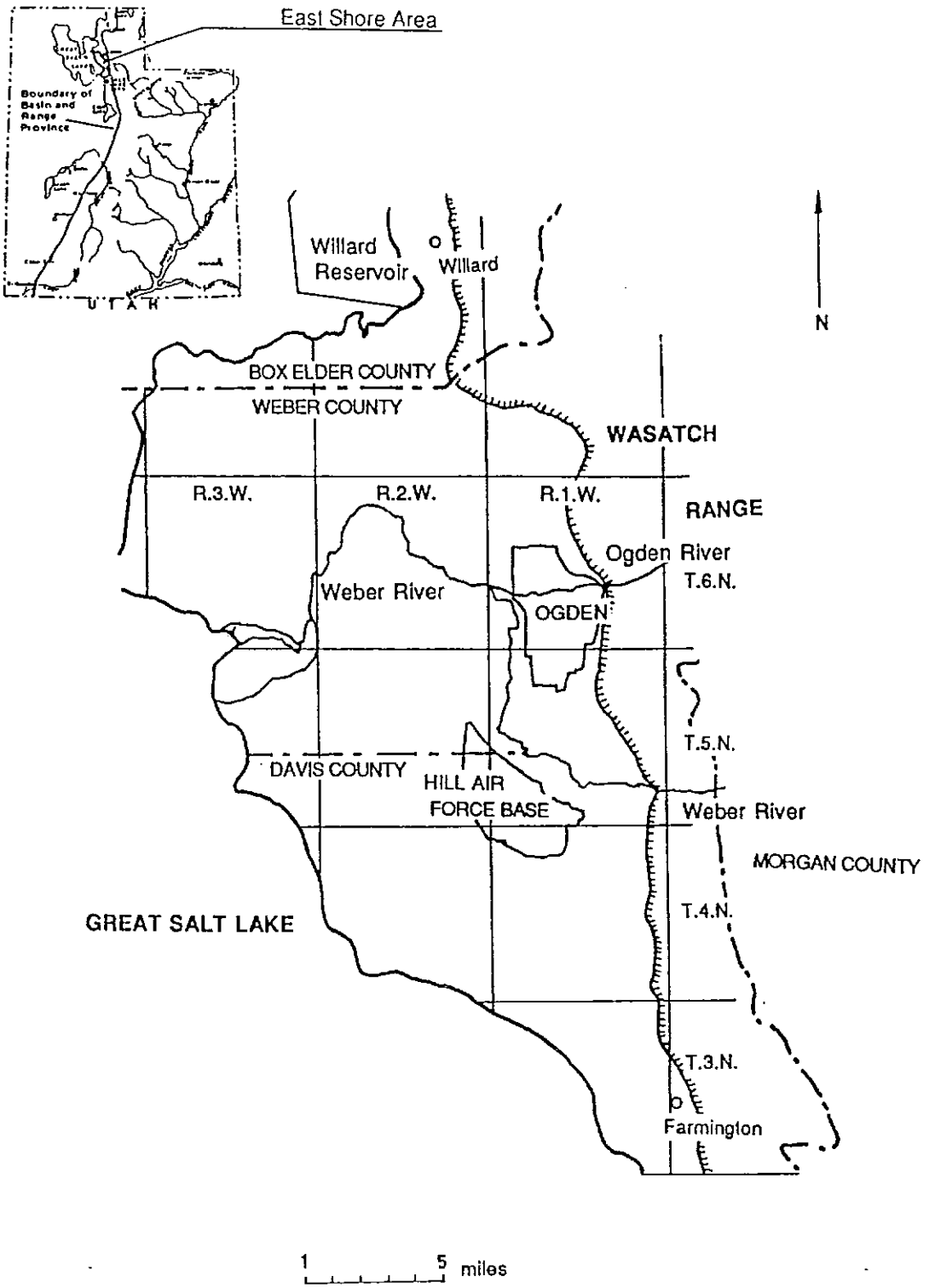

Fig. 1. Map of the East Shore Area, Utah

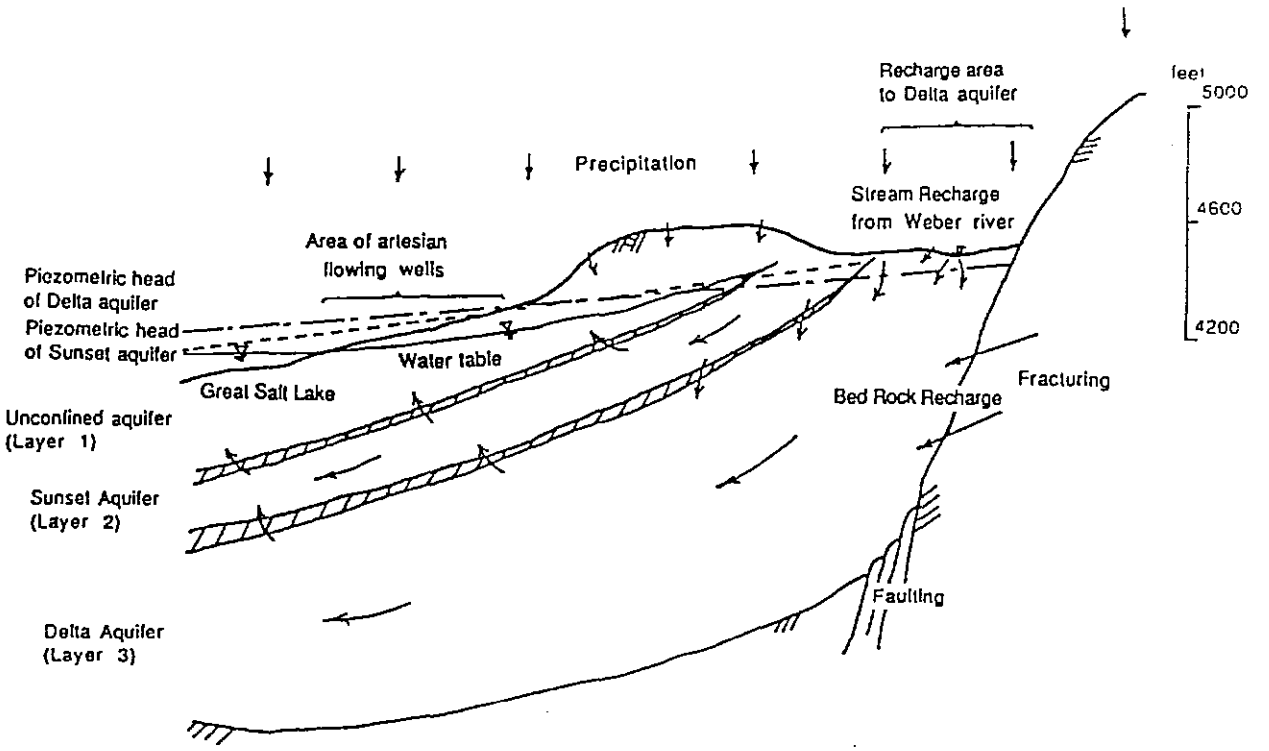

Fig. 2. Generalized profile of the East Shore Area aquifer system

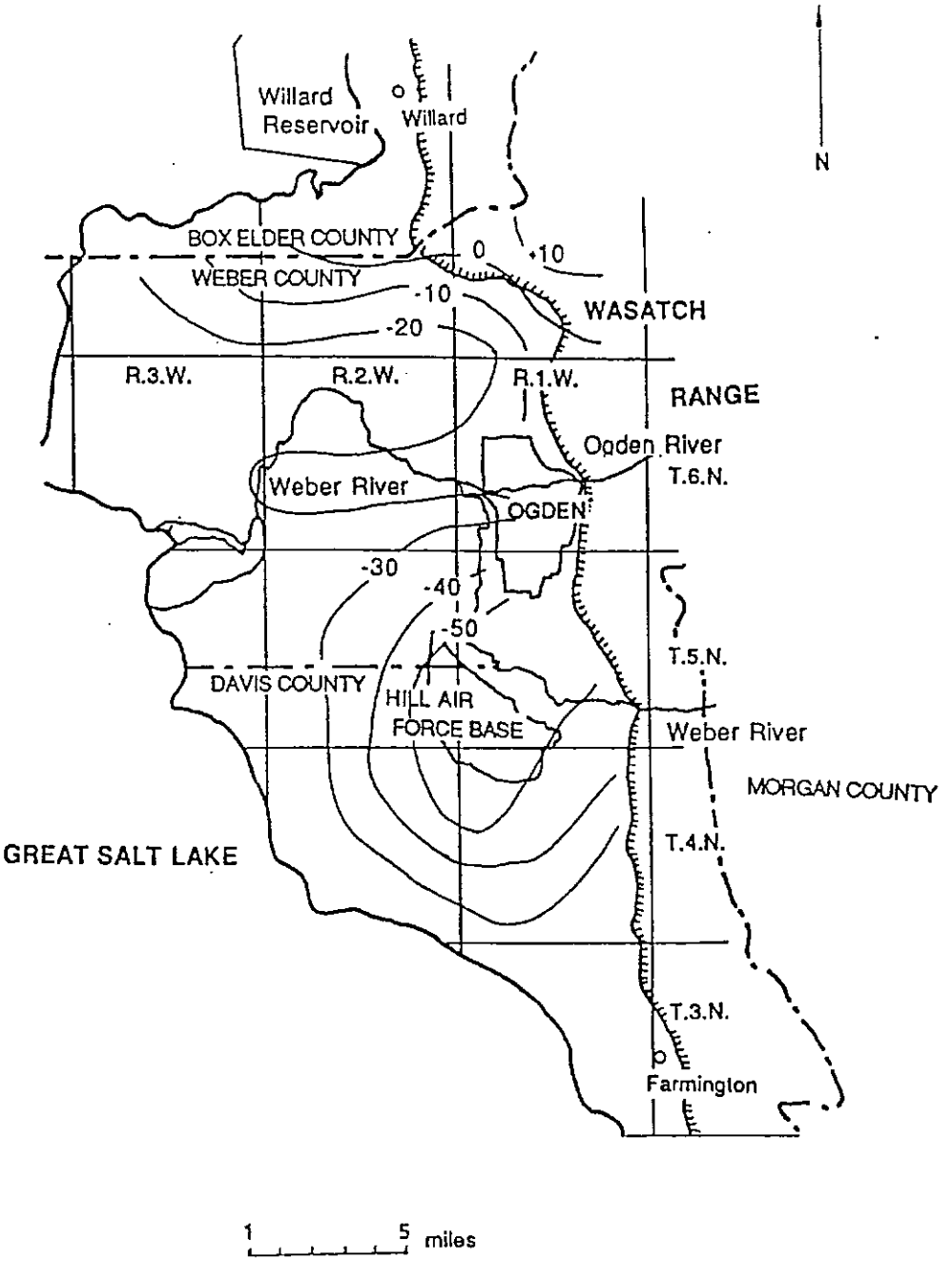

Fig. 3. Change of potentiometric heads of layer 3 (lower layer) from 1955 to 1985

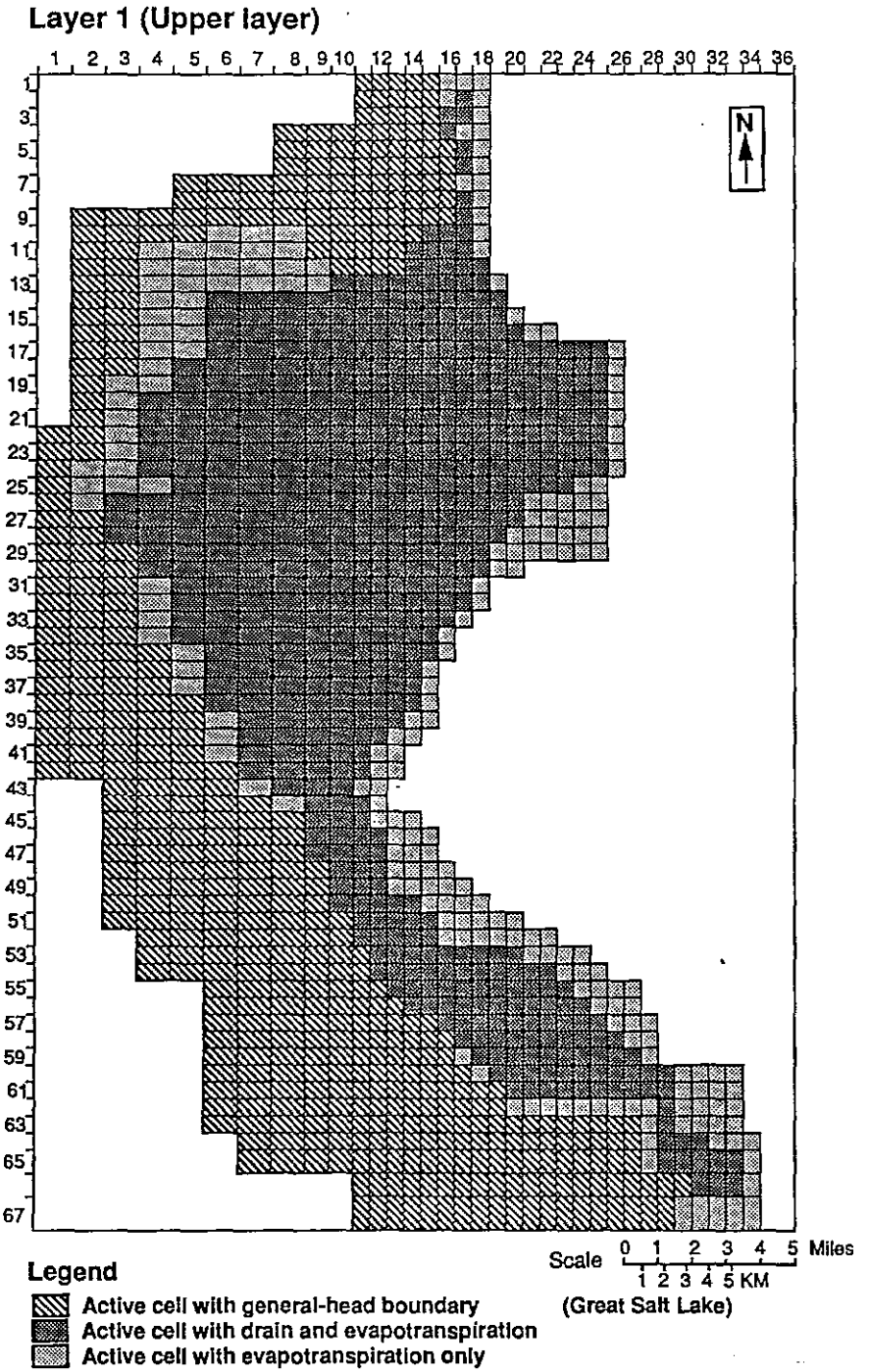

Fig. 4. Discretization of layer 1 (upper layer)

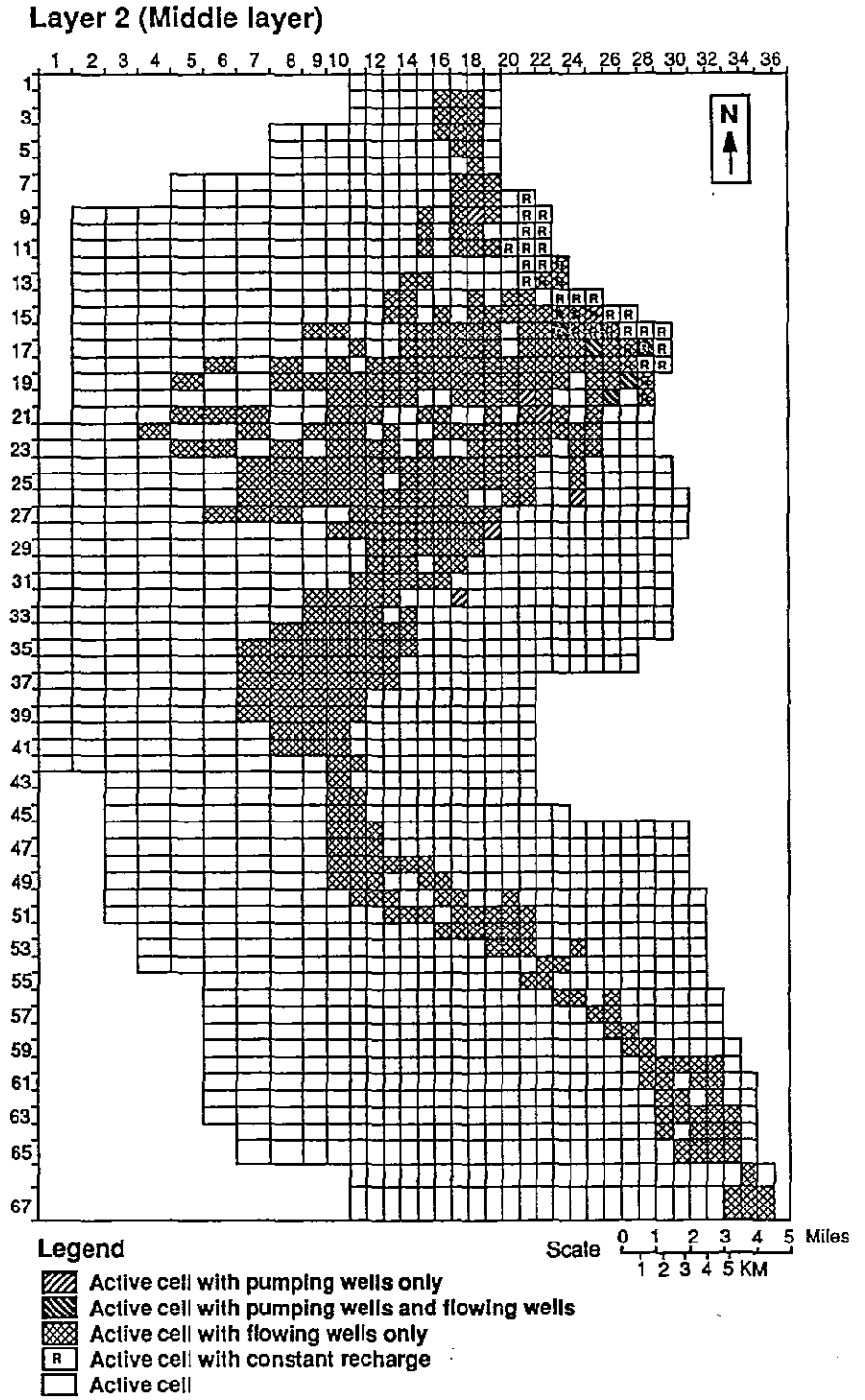

Fig. 5. Discretization of layer 2 (middle layer)

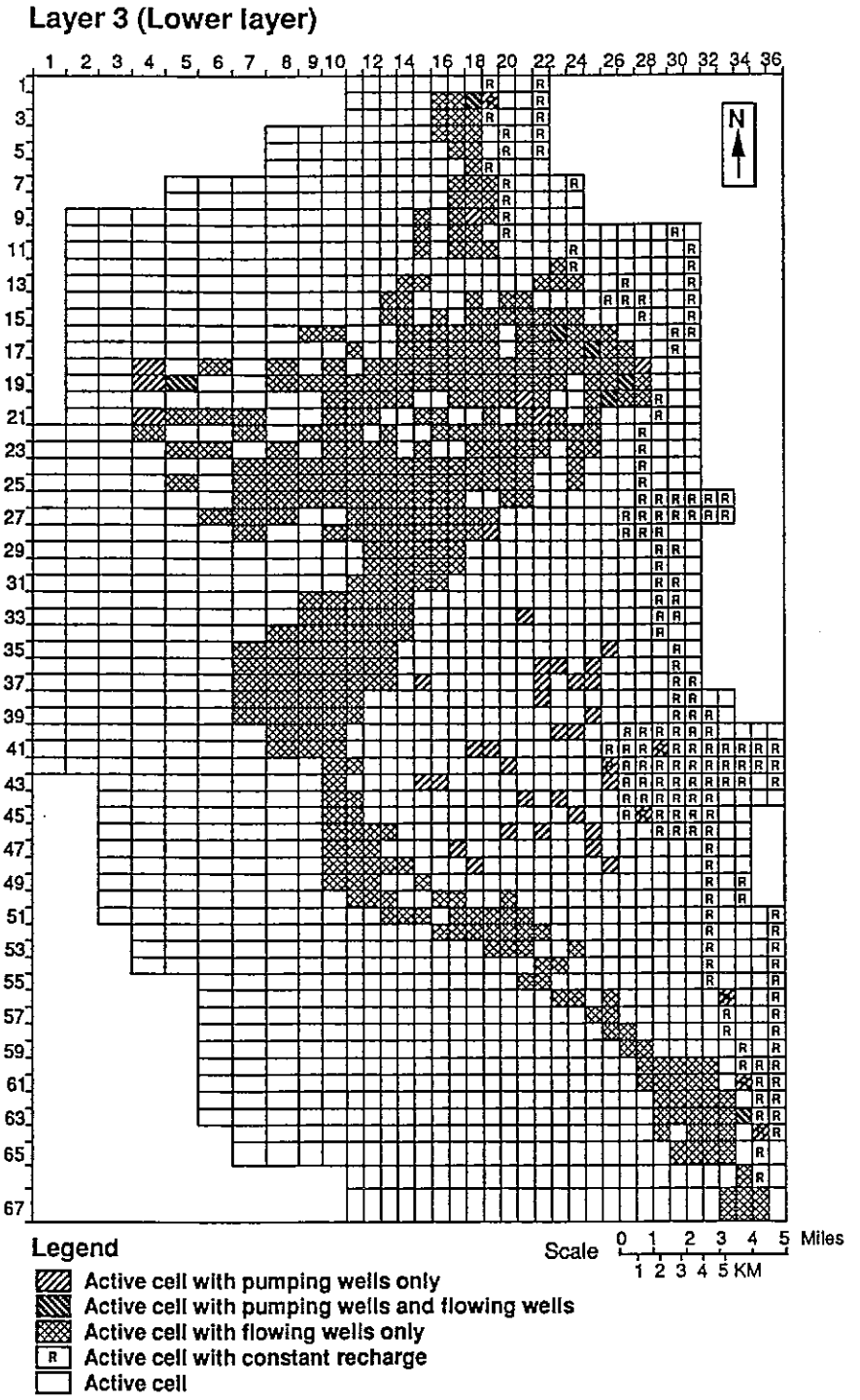

Fig. 6. Discretization of Layer 3 (lower layer)

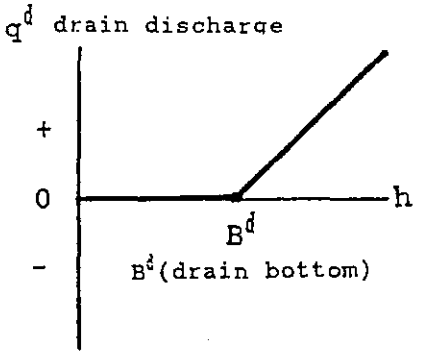

(a) Original equation

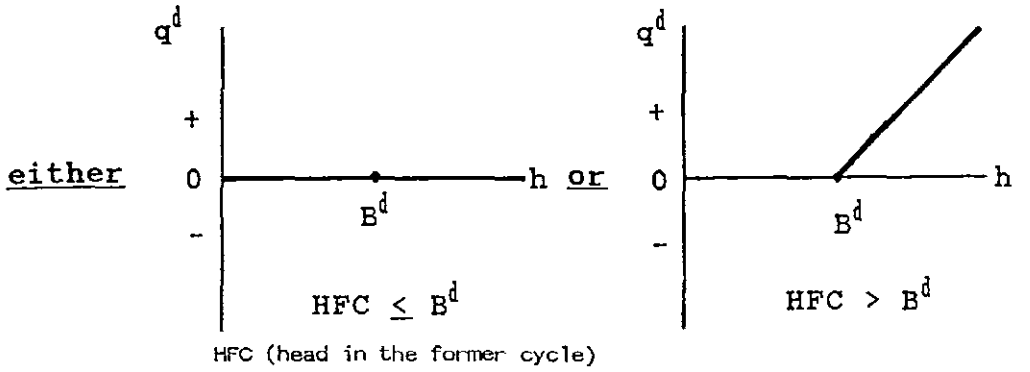

(b) In the original USUGWM

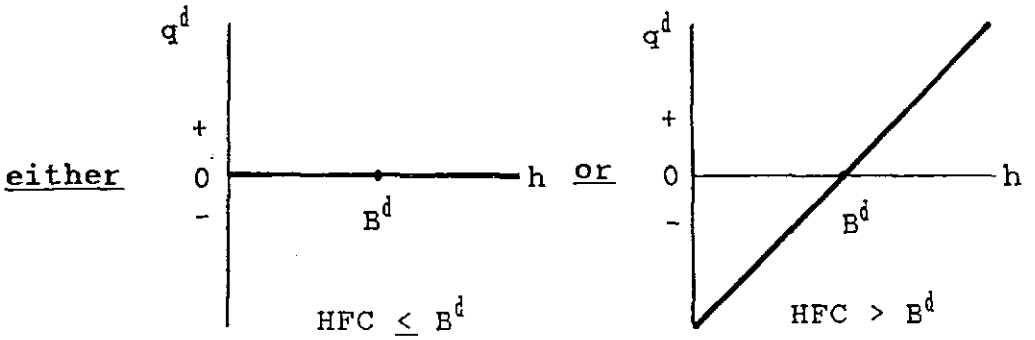

(c) In the modified USUGWM

Fig. 7. Linear formulae for discharge from drains

1. Original USUGWM

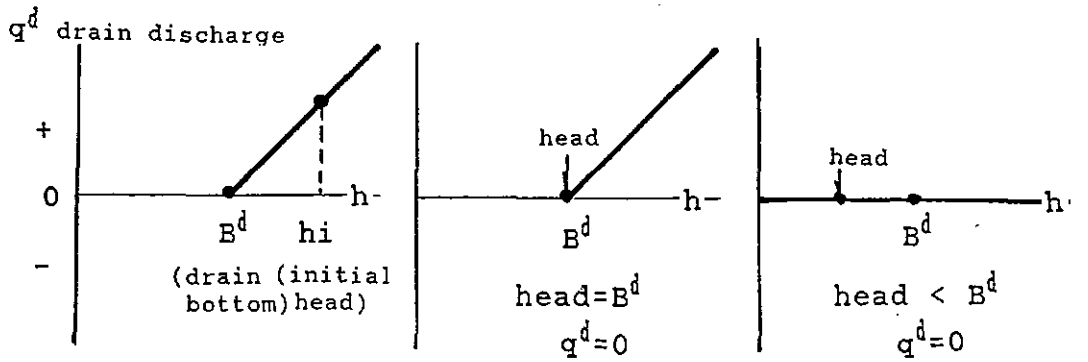

(a) Initial condition (b) 1st cycle (c) 2nd cycle

2. Modified USUGWM

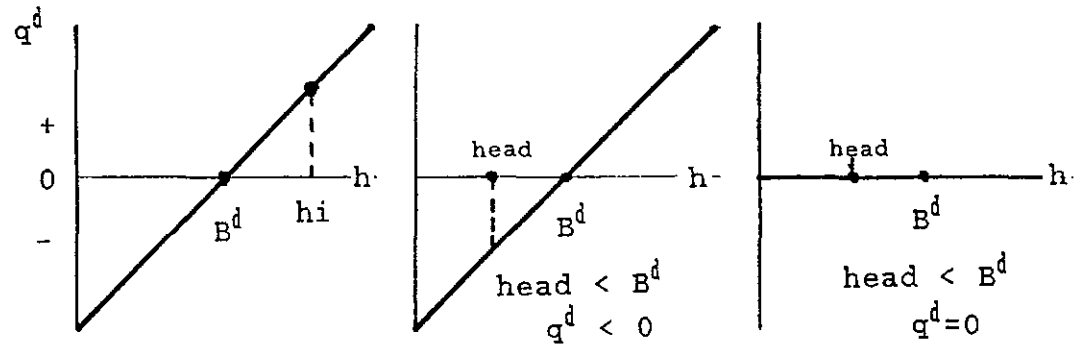

(d) Initial condition (e) 1st cycle (f) 2nd cycle

Fig. 8. Solving procedures for discharge from drains

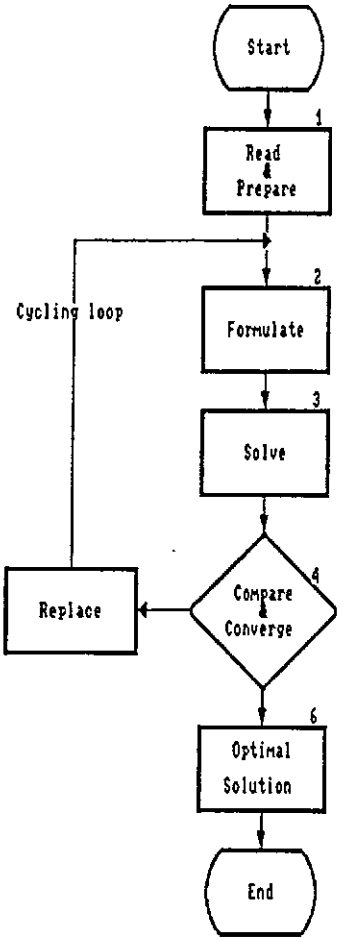

Embedding model

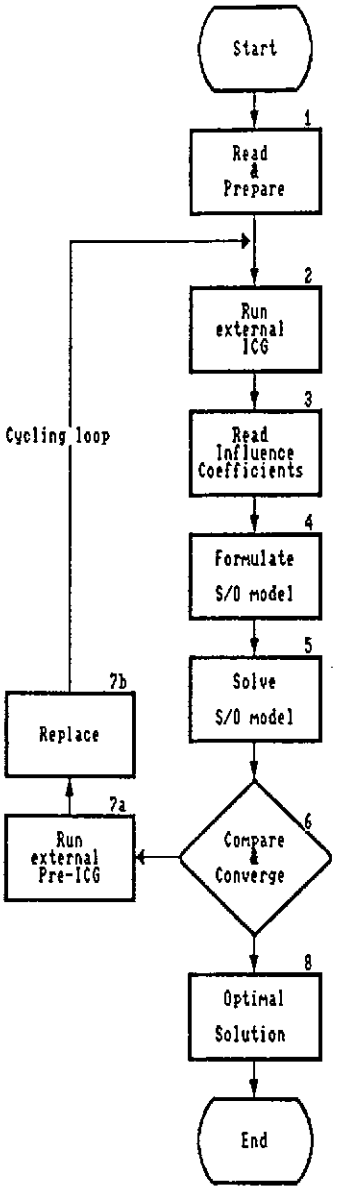

Response Matrix model

Fig. 9. Flow charts of solving procedures for the embedding and response matrix S/O models

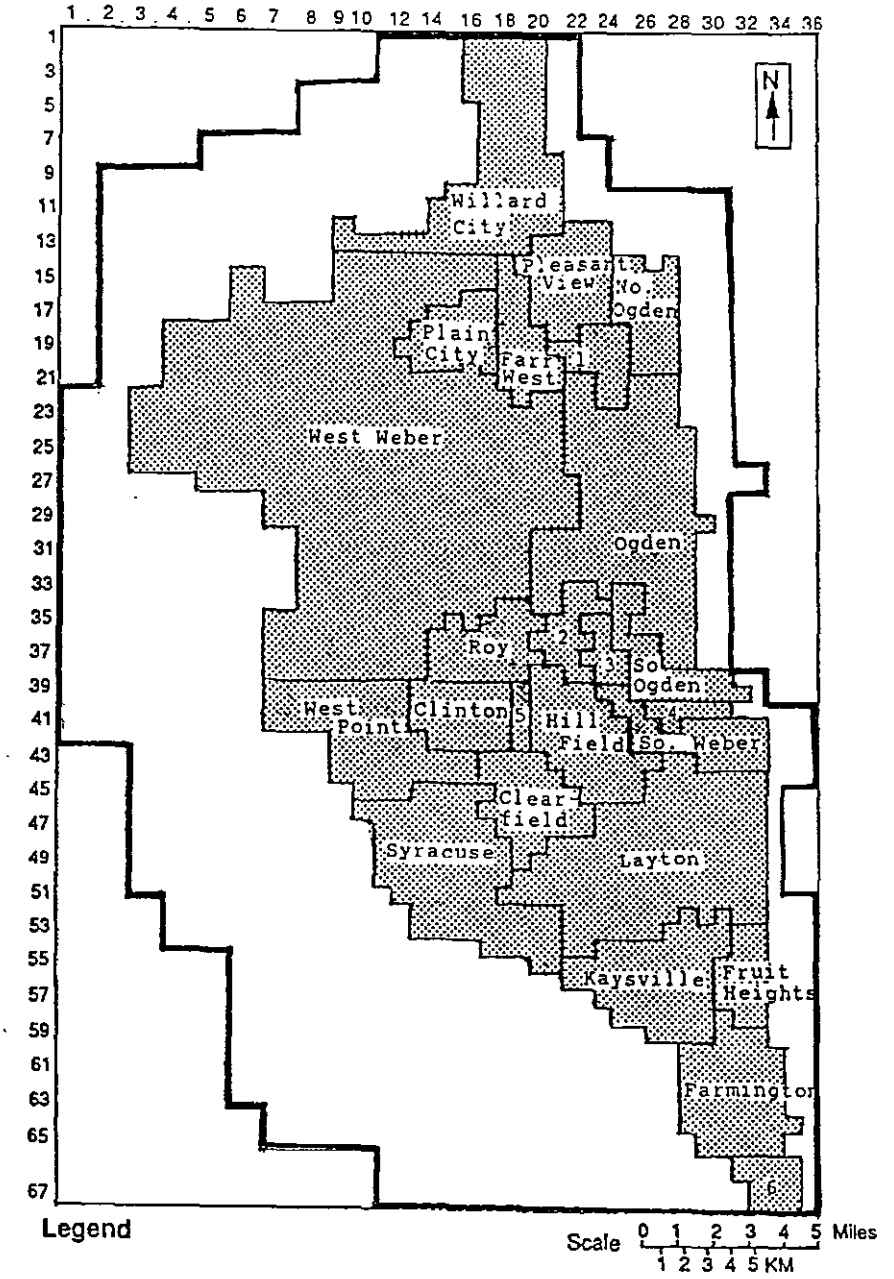

Fig. 10. Boundaries of water entities

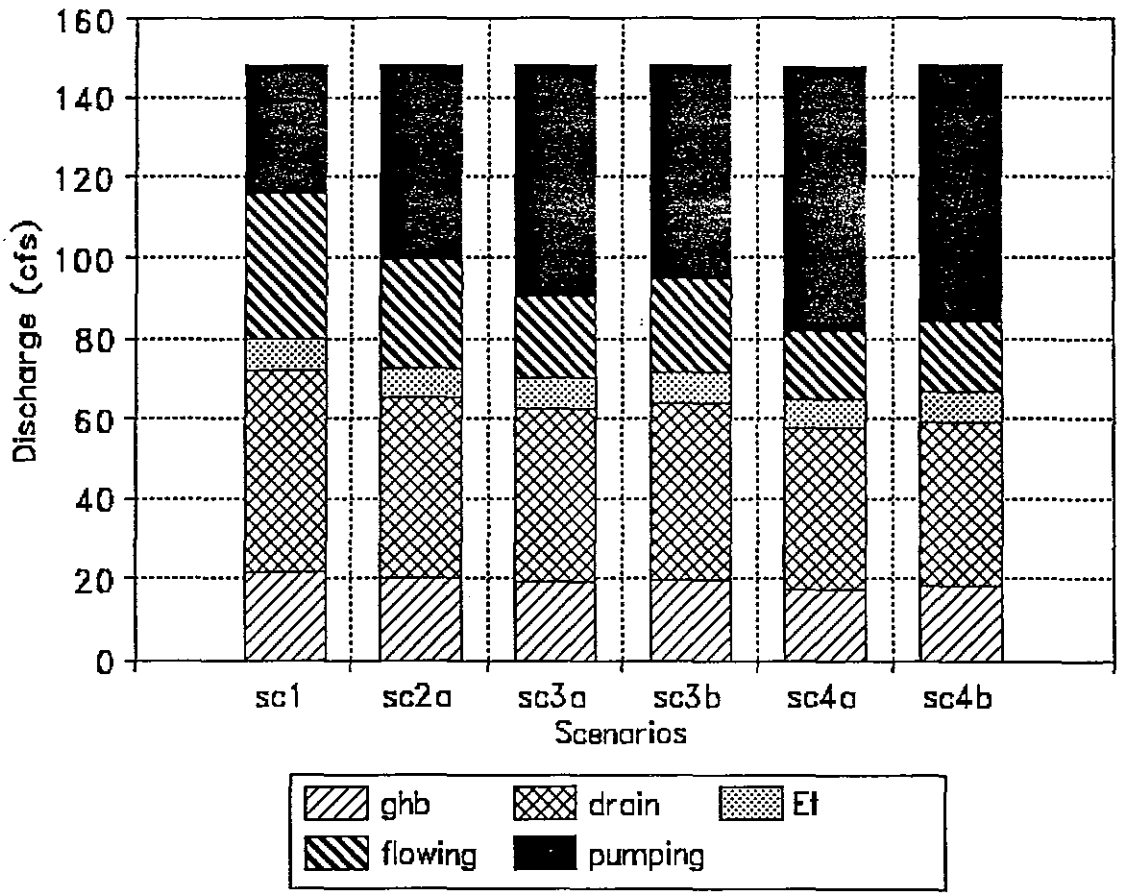

Fig. 11. Discharges for scenarios 1, 2a, 3a, 3b, 4a, and 4b.

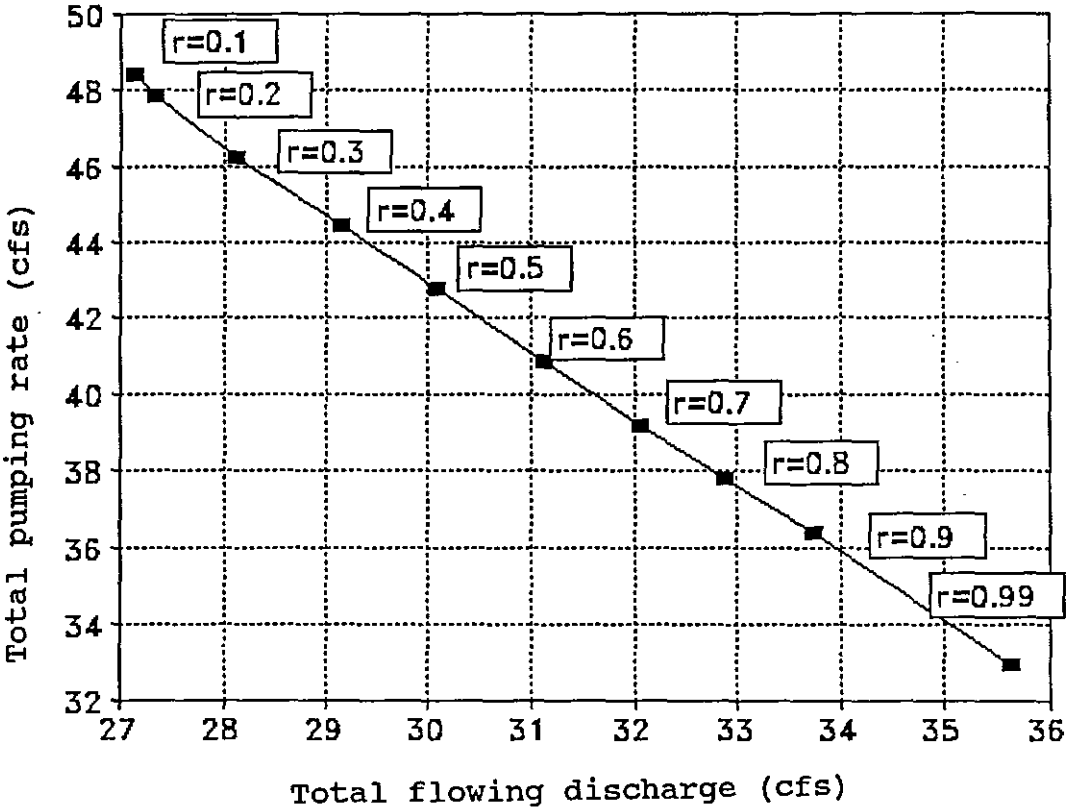

Fig. 12. Tradeoff curve between pumping and flowing wells

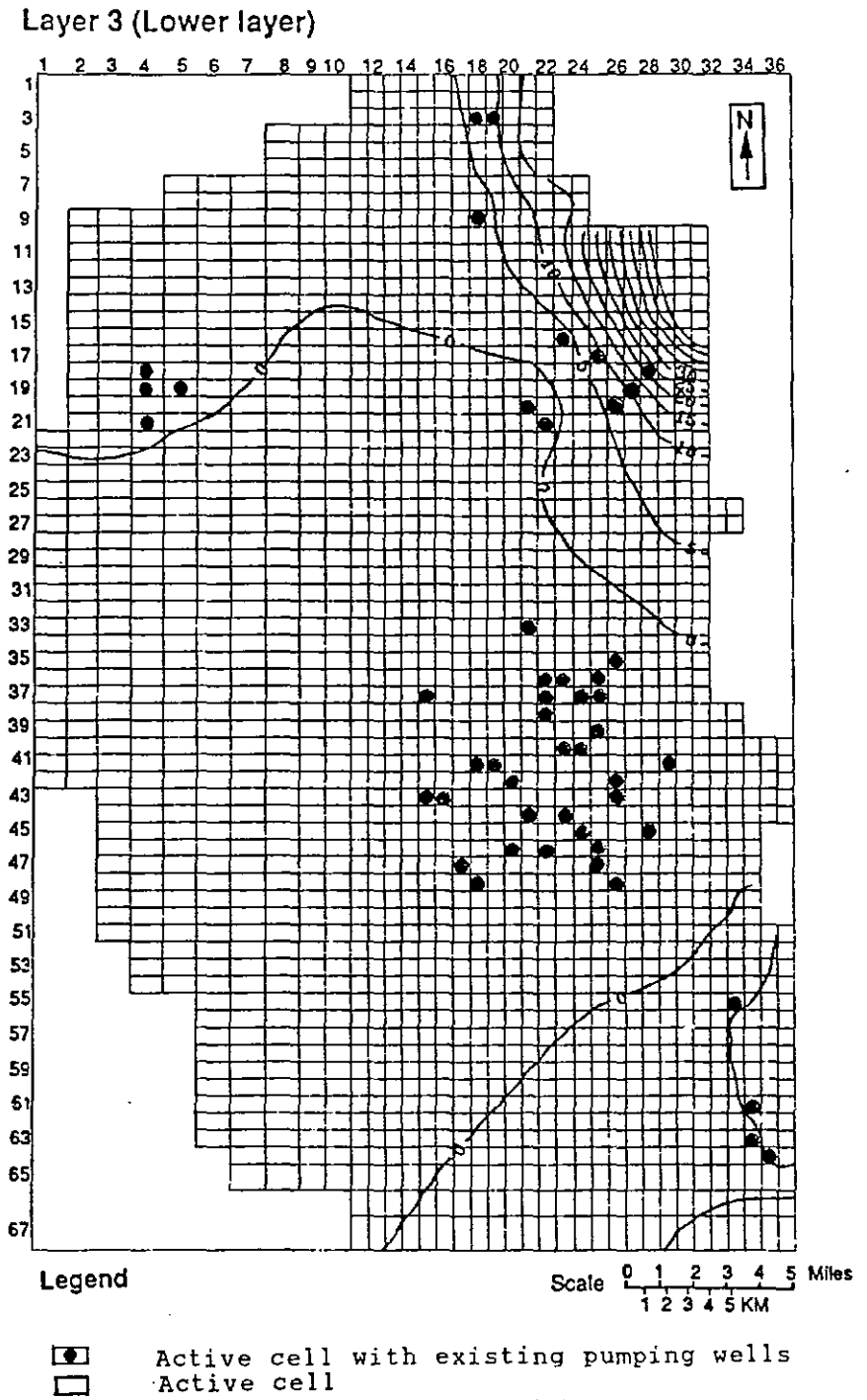

Fig. 13. Drawdown contours of scenario 1

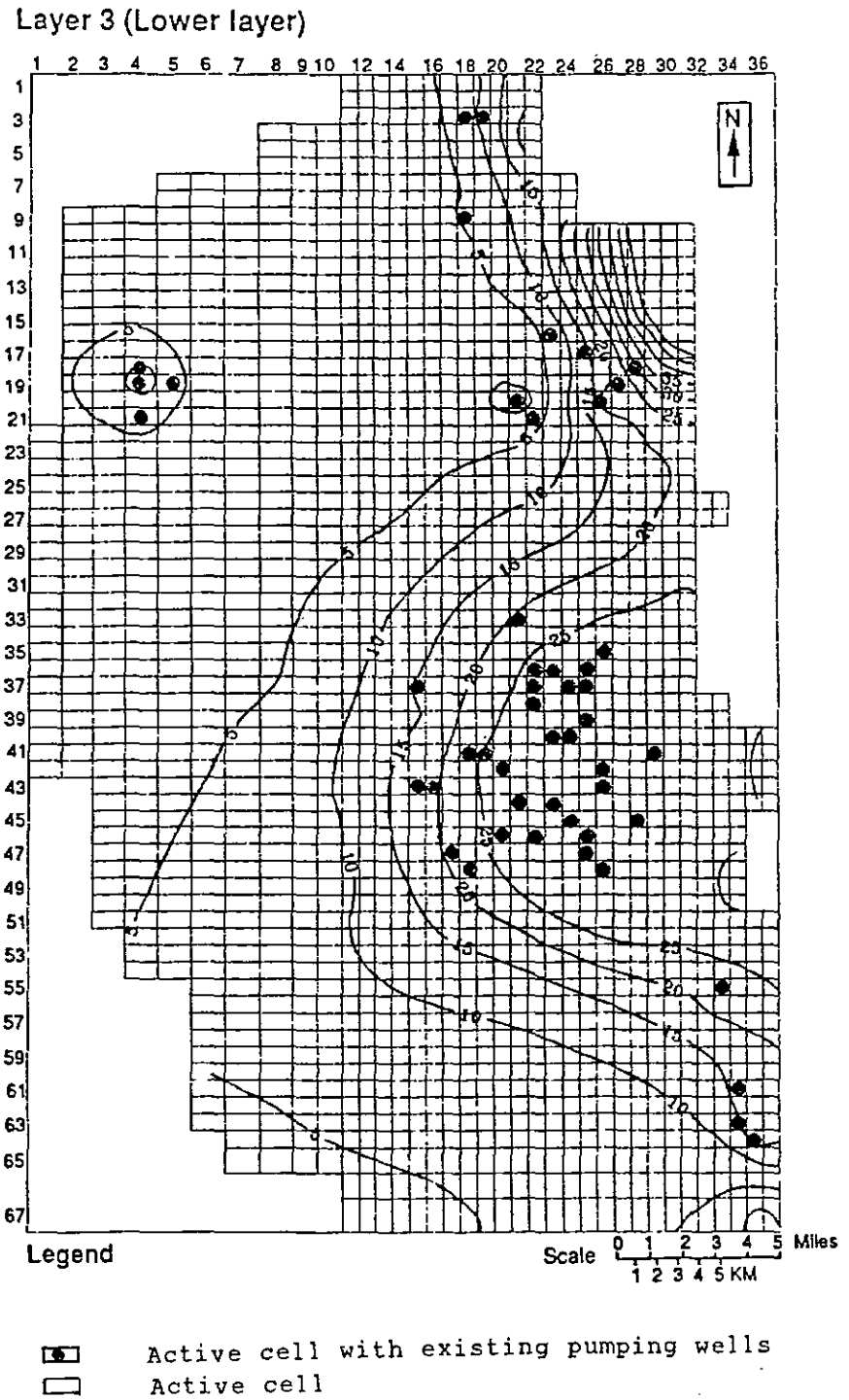

Fig. 14. Drawdown contours of scenario 2b (maximum allowable drawdown = 30 ft)

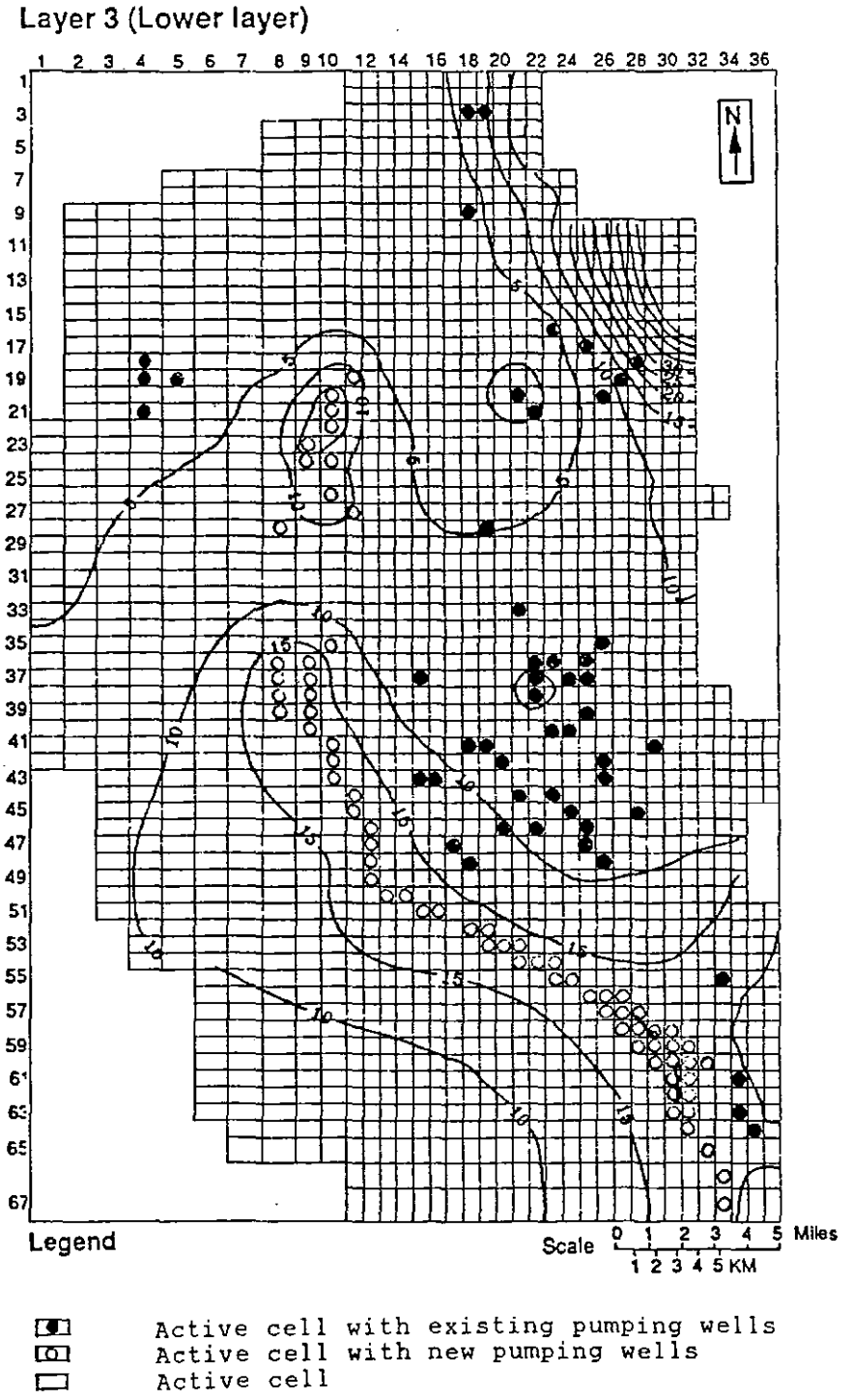

Fig. 15. Drawdown contours of scenario 4b

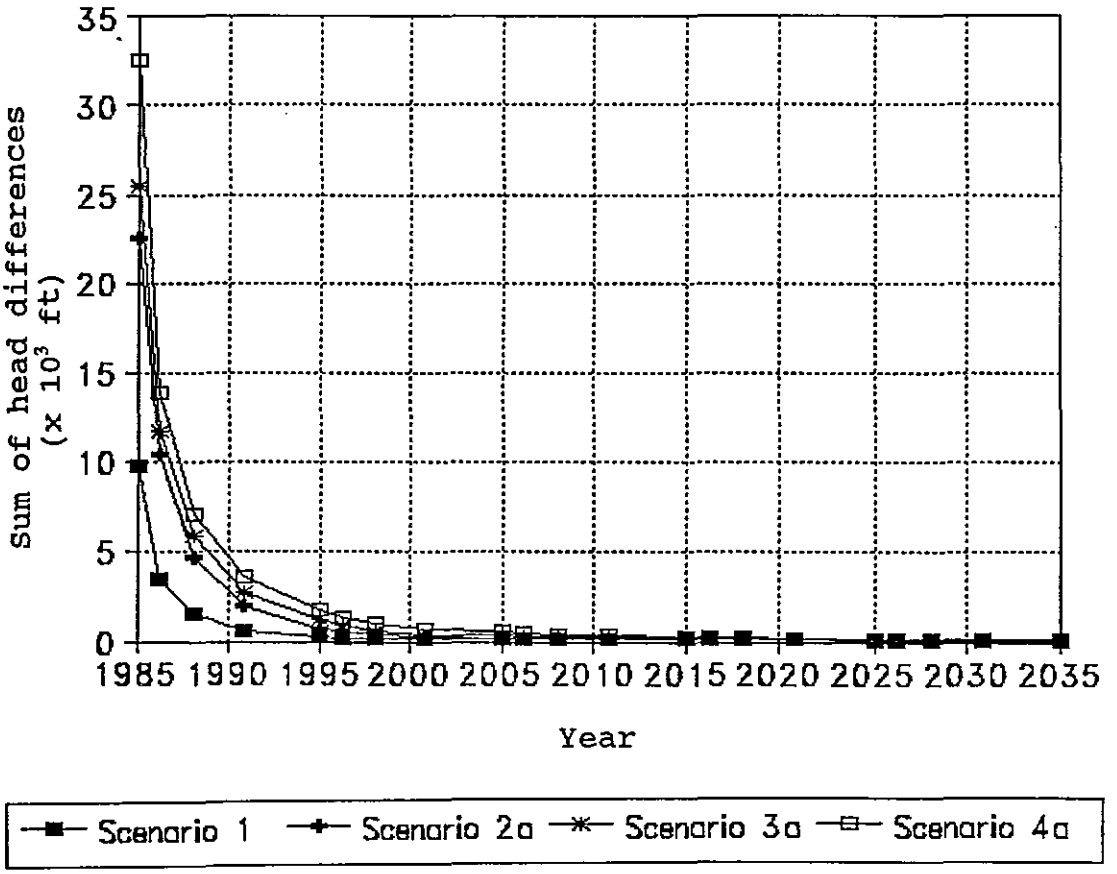

Fig. 16. Evolution of heads to the optimal steady-state